

Online Research @ Cardiff

This is an Open Access document downloaded from ORCA, Cardiff University's institutional repository: <https://orca.cardiff.ac.uk/id/eprint/135114/>

This is the author's version of a work that was submitted to / accepted for publication.

Citation for final published version:

Meng, Kun, Cui, Chunyi, Liang, Zhimeng, Li, Haijiang ORCID: <https://orcid.org/0000-0001-6326-8133> and Pei, Huafu 2020. A new approach for longitudinal vibration of a large-diameter floating pipe pile in visco-elastic soil considering the three-dimensional wave effects. Computers and Geotechnics 10.1016/j.compgeo.2020.103840 file

Publishers page: <https://doi.org/10.1016/j.compgeo.2020.103840>
<<https://doi.org/10.1016/j.compgeo.2020.103840>>

Please note:

Changes made as a result of publishing processes such as copy-editing, formatting and page numbers may not be reflected in this version. For the definitive version of this publication, please refer to the published source. You are advised to consult the publisher's version if you wish to cite this paper.

This version is being made available in accordance with publisher policies.

See

<http://orca.cf.ac.uk/policies.html> for usage policies. Copyright and moral rights for publications made available in ORCA are retained by the copyright holders.



Elsevier Editorial System(tm) for Computers
and Geotechnics

Manuscript Draft

Manuscript Number: COGE-D-20-00468R1

Title: A new approach for longitudinal vibration of a large-diameter floating pipe pile in visco-elastic soil considering the three-dimensional wave effects

Article Type: Research Paper

Keywords: three-dimensional axisymmetric model; floating pipe pile; analytical solution; radial wave effect; complex impedance

Corresponding Author: Professor Chunyi Cui, PHD

Corresponding Author's Institution: Dalian Maritime University, P.R.China

First Author: Kun Meng

Order of Authors: Kun Meng; Chunyi Cui; Zhimeng Liang; Haijiang Li; Huafu Pei

Abstract: A novel approach is presented to describe the dynamic interaction system of a large-diameter floating pipe pile and surrounding soils, taking the three-dimensional wave effects into account. The corresponding analytical solutions for longitudinal complex impedance are obtained and subsequently validated via comparisons with existing solutions. Comparative analyses are also performed to illustrate the difference between the present and previous solutions, concerning the wave propagation effect in the radial direction on the longitudinal dynamic vibration of pile shaft. Furthermore, the effects of Poisson's ratio and visco-elastic support beneath the pile toe, on the longitudinal dynamic vibration of pile shaft, are investigated. It is indicated that the presented approach and corresponding solutions provide a more wide-ranging application for longitudinal vibration analysis of a large-diameter floating pipe pile, which can also be reduced to analyze the longitudinal vibration problems of large-diameter floating solid pile and fixed-end pipe pile.

A new approach for longitudinal vibration of a large-diameter floating pipe pile in visco-elastic soil considering the three-dimensional wave effects

Kun Meng^{a,b}, Chunyi Cui^{a,*}, Zhimeng Liang^a, Haijiang Li^b, Huafu Pei^c

^a Department of Civil Engineering, Dalian Maritime University, Dalian, 116026, China

^b Cardiff School of Engineering, Cardiff University, Queen's Buildings, The Parade, Cardiff, Wales CF24 3AA, UK

^c Faculty of Infrastructure Engineering, Dalian University of Technology, Dalian, 116024, China

Abstract: A novel approach is presented to describe the dynamic interaction system of a large-diameter floating pipe pile and surrounding soils, taking the three-dimensional wave effects into account. The corresponding analytical solutions for longitudinal complex impedance are obtained and subsequently validated via comparisons with existing solutions. Comparative analyses are also performed to illustrate the difference between the present and previous solutions, concerning the wave propagation effect in the radial direction on the longitudinal dynamic vibration of pile shaft. Furthermore, the effects of Poisson's ratio and visco-elastic support beneath the pile toe, on the longitudinal dynamic vibration of pile shaft, are investigated. It is indicated that the presented approach and corresponding solutions provide a more wide-ranging application for longitudinal vibration analysis of a large-diameter floating pipe pile, which can also be reduced to analyze the longitudinal vibration problems of large-diameter floating solid pile and fixed- end pipe pile.

Keywords: three-dimensional axisymmetric model; floating pipe pile; analytical solution; radial wave effect; complex impedance

*Corresponding author at: Department of Civil Engineering, Dalian Maritime University, Liaoning, Dalian, 116026, China. E-mail address: cuichunyi@dmlu.edu.cn (C.Y. CUI)

1. Introduction

Pile foundations are commonly adopted to support structures in civil, coastal and offshore engineering, etc. Longitudinal vibration of piled structures due to vertical ground motion of earthquake, traffic and vibrating machinery is of great practical engineering significance for dynamic foundation design, earthquake-resistance design and pile dynamic testing [1-3]. Hence, the studies of

longitudinal vibration of pile have attracted extensive attention in recent decades [4-6].

Several analytical models have been proposed to discuss the longitudinal dynamic characteristics of soil-pile interaction system [7-9]. The Winkler model has been widely used due to its convenience, in which the soil is simplified into a series of spring-dashpot elements [10-12]. Nevertheless, the Winkler model cannot consider the wave propagation within the soils [13-15]. Novak [16] further presented a plane-strain model by assuming the soils as thin layers. However, the Novak's plane-strain model was unsatisfactory in a certain high-frequency range for neglecting the vertical wave propagation between thin layers [17]. Subsequently, Nogami et al. [18] developed a three-dimensional (3D) continuum model that considered the variations of vertical displacements, in both horizontal and longitudinal directions. Furthermore, Hu et al. [19] and Wu et al. [20] proposed more rigorous 3D continuum models of soil to discuss the longitudinal dynamic characteristics of solid pile.

In previous research, pile was commonly considered as a one-dimensional Euler-Bernoulli rod due to its simplicity [21-23]. In the Euler-Bernoulli rod-type model of pile, the assumption of plane section can lead to non-ignorable inaccuracy when the slenderness ratio of pile shaft is small [24]. In addition, some researchers [25-27] found that the Rayleigh-Love model of pile could improve the computational accuracy for longitudinal vibration problem under low-frequency excitation, by comparing with *the Euler-Bernoulli rod model*. Therefore, Wu et al. [28] presented their corresponding complex impedance solution for a tapered pile in soil by combining the Rayleigh-Love rod model and the plane-strain soil model, to take the large-diameter effect of pile on longitudinal vibration into account. Lu et al. [29, 30] considered both the 3D wave effect of soil and the large-diameter effect of pile shaft to discuss the coupled longitudinal dynamic characteristics of pile in longitudinal layered soils. Afterward, Li et al. [31] conducted further studies on the longitudinal dynamic characteristics of a large-diameter pile in layered soils with radial inhomogeneity. Zheng et al. [32] and Li et al. [33] also examined the longitudinal dynamic characteristics of pile in radially homogeneous and inhomogeneous soils, respectively, by extending the Rayleigh-Love rod theory to pipe piles.

Although the Rayleigh-Love rod model can approximately consider the lateral inertia effect comparing with *the Euler-Bernoulli rod model*, it is deduced from one-dimensional wave theory and the radial variations of stress and displacement of material particles, i.e. the 3D wave effect in the pile shaft are ignored. Fei et al. [34] have discussed the 3D wave effect on the reflected wave velocity of a large-diameter pipe pile under vertical low strain transient based on the 3D finite element model. Hence, Liu and Ding [35] employed a simplified model of large-diameter pipe rod with fixed support by assuming an even dynamic response along the radial direction. Ding et al. [36] further proposed an analytical model for a large-diameter pipe rod with fixed supports to investigate the 3D wave effect on dynamic response of rod shaft. Moreover, Liu et al. [37] proposed an analytical solution for a longitudinal dynamic

1 interaction system of end-bearing pipe pile and soils with fixed supports, which considered
 2 both the 3D wave propagation within pile shaft and soils. However, due to the assumption of
 3 the fixed supports beneath pile toe and soils, this proposed solution cannot be applied into the
 4 longitudinal dynamic analysis of a floating pipe pile in soils.
 5

6 Based on a wide-ranging literature review, it is evident that little attention has been
 7 attracted to the longitudinal vibration of a large-diameter floating pipe pile in visco-elastic soil
 8 considering the 3D wave effects within both pile shaft and soils. The primary aim of this
 9 paper is to present a new approach based on the 3D continuum wave propagation theory, to
 10 describe the longitudinal dynamic interaction system of a large-diameter floating pipe pile and
 11 soils, considering the visco-elastic supports beneath pile toe and soils. The displacements of
 12 both pile shaft and soils are to be determined by a derivation of the frequency transcendental
 13 equation corresponding to different vibration modes. Then, the analytical complex impedance
 14 solution for pile head is to be further derived by adopting the variable separation method and
 15 the fully coupled conditions of pipe pile and soils, which is reduced to verify its validity by
 16 comparisons with previous solutions. In addition, comparative analyses are to be conducted to
 17 investigate the effects of Poisson's ratio of pile and complex stiffness of visco-elastic supports
 18 on the longitudinal dynamic characteristics of coupled soil-pile system.
 19
 20
 21
 22
 23
 24
 25
 26
 27

28 2. The mechanical model

29 Fig.1 shows the 3D axisymmetric simplified mechanical model of the coupled dynamic
 30 interaction system of a floating pipe pile and surrounding soils under harmonic excitation.
 31 The length, inner, and outer diameters of the pipe pile are H , r_0 , and r_1 , respectively. The
 32 harmonic uniformly distributed excitation pressure is $\tilde{F}_0 e^{i\omega t}$, where $i = \sqrt{-1}$ is the imaginary
 33 unit and ω is circular frequency. The corresponding constants of visco-elastic supports
 34 beneath the pile toe and soils are k^P, δ^P and k^S, δ^S , respectively.
 35
 36
 37
 38
 39
 40
 41
 42
 43
 44
 45
 46
 47
 48
 49
 50
 51
 52
 53
 54
 55
 56
 57
 58
 59
 60
 61
 62
 63
 64
 65

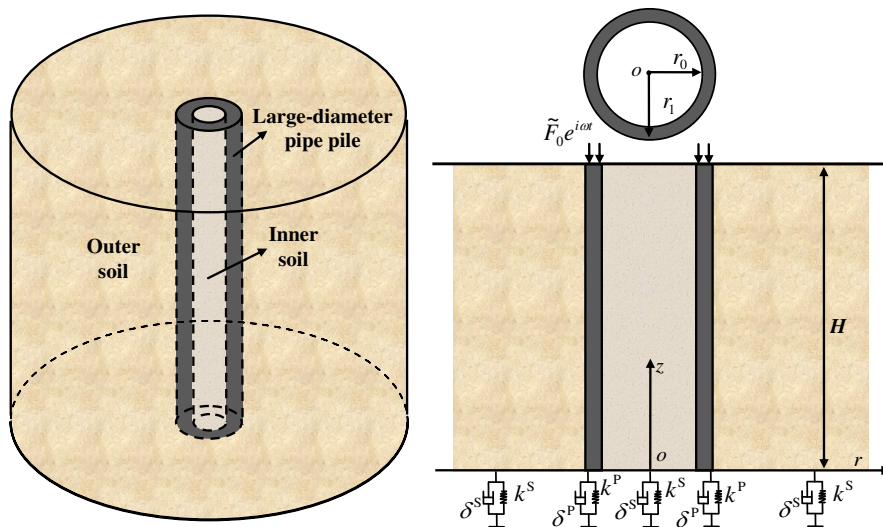


Fig. 1 The simplified mechanical model

The following assumptions are specified in the simplified mechanical model:

- (1) The pipe pile is considered as a linear elastic continuum with an annular uniform cross-section.
- (2) *The inner and outer soils are linear visco-elastic continuums with hysteretic-type material damping [38], which neglect the variation of shear modulus and damping of the soil with the shear strain level.*
- (3) The top surfaces of soils are free, namely, the normal stress and shear stress are zero. The excitation at the pile head is uniform harmonic pressure.
- (4) The visco-elastic supports beneath pile toe and soils are simplified as the Kelvin-Voigt model [15].
- (5) *The intensity of excitation force at the pile head is low and the deformations of soil-pile system are small. The interface sliding between the pile and soil is not considered [39-42]. It should be noted that, if the intensity of excitation force at the pile head is high, the proposed analytical model may overestimate both the stiffness and damping of pile due to the assumption of perfect bonding between pile and soil [43].*
- (6) *The proposed analytical approach in this paper is suitable for PCC piles [44] where the inner pipe is fully plugged [33, 45-47].*

According to the wave propagation theory of 3D continuums, the 3D axisymmetric governing equations of inner soil, outer soil, and pile shaft are established as follows.

$$(\lambda^{S_0} + \mu^{S_0}) \frac{\partial^2 u^{S_0}}{\partial z^2} + \mu^{S_0} \nabla^2 u^{S_0} = \rho^{S_0} \frac{\partial^2 u^{S_0}}{\partial t^2} \quad (1a)$$

$$(\lambda^{S_1} + \mu^{S_1}) \frac{\partial^2 u^{S_1}}{\partial z^2} + \mu^{S_1} \nabla^2 u^{S_1} = \rho^{S_1} \frac{\partial^2 u^{S_1}}{\partial t^2} \quad (1b)$$

$$(\lambda^P + G^P) \frac{\partial^2 u^P}{\partial z^2} + G^P \nabla^2 u^P = \rho^P \frac{\partial^2 u^P}{\partial t^2} \quad (1c)$$

where $\nabla^2 = \frac{\partial^2}{\partial r^2} + \frac{1}{r} \frac{\partial}{\partial r} + \frac{\partial^2}{\partial z^2}$; u^P , u^{S_0} and u^{S_1} are the longitudinal displacements of pipe pile, inner and outer soils, respectively; λ^{S_0} , μ^{S_0} and ρ^{S_0} are the Lamé constant, complex shear modulus, and density, respectively, of inner soil; λ^{S_1} , μ^{S_1} and ρ^{S_1} are the Lamé constant, complex shear modulus and density, respectively, of outer soil; λ^P , G^P and ρ^P denote the Lamé constant, shear modulus, and density, respectively, of pipe pile. \tilde{u}^P , \tilde{u}^{S_0} and \tilde{u}^{S_1} are the displacement amplitudes of pipe pile, inner and outer soils, respectively.

For the excitation force is harmonic, the vertical displacements of pipe pile, inner and outer soils can be written as $u^P = \tilde{u}^P e^{i\omega t}$, $u^{S_0} = \tilde{u}^{S_0} e^{i\omega t}$ and $u^{S_1} = \tilde{u}^{S_1} e^{i\omega t}$, respectively. Then, Eq. (1a)~Eq. (1c) can be expressed as the following forms, respectively,

$$(1 + 2\xi^{S_0}i)\nabla^2\tilde{u}^{S_0} + \frac{1 + 2\xi^{S_0}i}{1 - 2\nu^{S_0}} \frac{\partial^2\tilde{u}^{S_0}}{\partial z^2} = -\left(\frac{\omega}{V^{S_0}}\right)^2\tilde{u}^{S_0} \quad (2a)$$

$$(1 + 2\xi^{S_1}i)\nabla^2\tilde{u}^{S_1} + \frac{1 + 2\xi^{S_1}i}{1 - 2\nu^{S_1}} \frac{\partial^2\tilde{u}^{S_1}}{\partial z^2} = -\left(\frac{\omega}{V^{S_1}}\right)^2\tilde{u}^{S_1} \quad (2b)$$

$$\nabla^2\tilde{u}^P + \frac{1}{1 - 2\nu^P} \frac{\partial^2\tilde{u}^P}{\partial z^2} = -\left(\frac{\omega}{V^P}\right)^2\tilde{u}^P \quad (2c)$$

where ξ^{S_0} and ξ^{S_1} denote the hysteretic damping ratio of inner and outer soils, respectively.

ν^P , ν^{S_0} and ν^{S_1} are Poisson's ratio of pile, inner and outer soils, respectively.

$V^P = \sqrt{G^P/\rho^P}$, $V^{S_0} = \sqrt{G^{S_0}/\rho^{S_0}}$ and $V^{S_1} = \sqrt{G^{S_1}/\rho^{S_1}}$ are the shear wave velocity of pile,

inner and outer soils, respectively. $G^{S_0} = \mu^{S_0}/(1 + 2\xi^{S_0}i)$ and $G^{S_1} = \mu^{S_1}/(1 + 2\xi^{S_1}i)$ are shear modulus of inner and outer soils, respectively.

The boundary conditions of the simplified mechanical model are illustrated as follows:

The normal stresses at the free top surfaces of inner and outer soils are zero,

$$\left. \frac{\partial\tilde{u}^{S_0}}{\partial z} \right|_{z=H} = 0 \quad (3a)$$

$$\left. \frac{\partial\tilde{u}^{S_1}}{\partial z} \right|_{z=H} = 0 \quad (3b)$$

The boundary conditions at the bottom of inner and outer soils are shown as follows:

$$\left. \frac{\partial\tilde{u}^{S_0}}{\partial z} + \frac{k^S + i\omega\delta^S}{E^{S_0}}\tilde{u}^{S_0} \right|_{z=0} = 0 \quad (4a)$$

$$\left. \frac{\partial\tilde{u}^{S_1}}{\partial z} + \frac{k^S + i\omega\delta^S}{E^{S_1}}\tilde{u}^{S_1} \right|_{z=0} = 0 \quad (4b)$$

where E^{S_0} and E^{S_1} are the elastic modulus of inner soil and outer soil, respectively. \tilde{u}^{S_0}

is a limited value when $r = 0$. \tilde{u}^{S_1} diminishes to zero at infinity, namely,

$$\lim_{r \rightarrow 0} \tilde{u}^{S_0} < \infty \quad (5a)$$

$$\lim_{r \rightarrow \infty} \tilde{u}^{S_1} = 0 \quad (5b)$$

The boundary conditions of pipe pile are expressed as the following forms,

$$G^P \frac{2 - 2\nu^P}{1 - 2\nu^P} \left. \frac{\partial\tilde{u}^P}{\partial z} \right|_{z=H} = \tilde{F}_0 \quad (6a)$$

$$\left. \frac{\partial\tilde{u}^P}{\partial z} + \frac{k^P + i\omega\delta^P}{E^P}\tilde{u}^P \right|_{z=0} = 0 \quad (6b)$$

where E^P is the elastic modulus of pipe pile.

The shear stress equilibrium and displacements continuity conditions of soil-pile system are

$$\tilde{u}^P = \tilde{u}^{S_0} \Big|_{r=r_0} \quad (7a)$$

$$\tilde{u}^P = \tilde{u}^{S_1} \Big|_{r=r_1} \quad (7b)$$

$$\tilde{\tau}^P = \tilde{\tau}^{S_0} \Big|_{r=r_0} \quad (7c)$$

$$\tilde{\tau}^P = \tilde{\tau}^{S_1} \Big|_{r=r_1} \quad (7d)$$

where $\tilde{\tau}^P$, $\tilde{\tau}^{S_0}$ and $\tilde{\tau}^{S_1}$ denote the shear stress of pipe pile, inner soil and outer soil, respectively.

3. Solutions of the governing equations

3.1 Longitudinal vibration of soils

Using the method of separation variables, \tilde{u}^{S_0} and \tilde{u}^{S_1} can be expressed as $\tilde{u}^{S_0}(r, z) = R^{S_0}(r)Z^{S_0}(z)$ and $\tilde{u}^{S_1}(r, z) = R^{S_1}(r)Z^{S_1}(z)$, respectively. Then, Eq. (2a) and Eq. (2b) can be rewritten as:

$$(1 + 2\xi^{S_0}i) \left(\frac{d^2 R^{S_0}}{R^{S_0} dr^2} + \frac{d^2 R^{S_0}}{rR^{S_0} dr^2} \right) + \left(\frac{1 + 2\xi^{S_0}i}{1 - 2\nu^{S_0}} + 1 \right) \frac{d^2 Z^{S_0}}{Z^{S_0} dz^2} = -\left(\frac{\omega}{V^{S_0}} \right)^2 \quad (8a)$$

$$(1 + 2\xi^{S_1}i) \left(\frac{d^2 R^{S_1}}{R^{S_1} dr^2} + \frac{d^2 R^{S_1}}{rR^{S_1} dr^2} \right) + \left(\frac{1 + 2\xi^{S_1}i}{1 - 2\nu^{S_1}} + 1 \right) \frac{d^2 Z^{S_1}}{Z^{S_1} dz^2} = -\left(\frac{\omega}{V^{S_1}} \right)^2 \quad (8b)$$

Thus, $(1 + 2\xi^{S_0}i) \left(\frac{d^2 R^{S_0}}{R^{S_0} dr^2} + \frac{d^2 R^{S_0}}{rR^{S_0} dr^2} \right)$, $\left(\frac{1 + 2\xi^{S_0}i}{1 - 2\nu^{S_0}} + 1 \right) \frac{d^2 Z^{S_0}}{Z^{S_0} dz^2}$, $(1 + 2\xi^{S_1}i) \left(\frac{d^2 R^{S_1}}{R^{S_1} dr^2} + \frac{d^2 R^{S_1}}{rR^{S_1} dr^2} \right)$ and $\left(\frac{1 + 2\xi^{S_1}i}{1 - 2\nu^{S_1}} + 1 \right) \frac{d^2 Z^{S_1}}{Z^{S_1} dz^2}$ are constants.

Setting $\frac{d^2 Z^{S_0}}{Z^{S_0} dz^2} = -(h^{S_0})^2$ as well as $\frac{d^2 Z^{S_1}}{Z^{S_1} dz^2} = -(h^{S_1})^2$ and substituting them into

Eqs.(8a) and (8b), respectively, it yields:

$$\frac{d^2 R^{S_0}}{R^{S_0} dr^2} + \frac{d^2 R^{S_0}}{rR^{S_0} dr^2} = \frac{\left[\frac{(1 + 2\xi^{S_0}i)(2 - 2\nu^{S_0})}{(1 - 2\nu^{S_0})} \right] (h^{S_0})^2 - \left(\frac{\omega}{V^{S_0}} \right)^2}{1 + 2\xi^{S_0}i} \quad (9a)$$

$$\frac{d^2 R^{S_1}}{R^{S_1} dr^2} + \frac{d^2 R^{S_1}}{rR^{S_1} dr^2} = \frac{\left[\frac{(1 + 2\xi^{S_1}i)(2 - 2\nu^{S_1})}{(1 - 2\nu^{S_1})} \right] (h^{S_1})^2 - \left(\frac{\omega}{V^{S_1}} \right)^2}{1 + 2\xi^{S_1}i} \quad (9b)$$

Therefore, Eqs.(8a) and (8b) can be further rewritten as:

$$\begin{cases} \frac{d^2 Z^{S_0}}{dz^2} + (h^{S_0})^2 Z^{S_0} = 0 \\ \frac{d^2 R^{S_0}}{dr^2} + \frac{1}{r} \frac{dR^{S_0}}{dr} - (q^{S_0})^2 R^{S_0} = 0 \end{cases} \quad (10a)$$

$$\begin{cases} \frac{d^2 Z^{S_1}}{dz^2} + (h^{S_1})^2 Z^{S_1} = 0 \\ \frac{d^2 R^{S_1}}{dr^2} + \frac{1}{r} \frac{dR^{S_1}}{dr} - (q^{S_1})^2 R^{S_1} = 0 \end{cases} \quad (10b)$$

where h^{S_0} , q^{S_0} , h^{S_1} and q^{S_1} satisfy the following expressions.

$$(q^{S_0})^2 = \frac{\left[\frac{(1+2\xi^{S_0}i)(2-2\nu^{S_0})}{(1-2\nu^{S_0})} \right] (h^{S_0})^2 - \left(\frac{\omega}{V^{S_0}} \right)^2}{1+2\xi^{S_0}i} \quad (11a)$$

$$(q^{S_1})^2 = \frac{\left[\frac{(1+2\xi^{S_1}i)(2-2\nu^{S_1})}{(1-2\nu^{S_1})} \right] (h^{S_1})^2 - \left(\frac{\omega}{V^{S_1}} \right)^2}{1+2\xi^{S_1}i} \quad (11b)$$

The general solutions of Eqs. (10a) and (10b) are obtained as

$$\begin{cases} Z^{S_0}(z) = C^{S_0} \cos(h^{S_0}z) + D^{S_0} \sin(h^{S_0}z) \\ R^{S_0}(r) = M^{S_0} K_0(q^{S_0}r) + N^{S_0} I_0(q^{S_0}r) \end{cases} \quad (12a)$$

$$\begin{cases} Z^{S_1}(z) = C^{S_1} \cos(h^{S_1}z) + D^{S_1} \sin(h^{S_1}z) \\ R^{S_1}(r) = M^{S_1} K_0(q^{S_1}r) + N^{S_1} I_0(q^{S_1}r) \end{cases} \quad (12b)$$

where C^{S_0} , D^{S_0} , M^{S_0} , N^{S_0} , C^{S_1} , D^{S_1} , M^{S_1} , and N^{S_1} are all undetermined coefficients. $I_0(\cdot)$ and $K_0(\cdot)$ are the first and second kind, respectively, modified Bessel functions of order zero.

Thus, substituting Eq.(12a) into Eqs.(3a) and (4a) as well as substituting Eq.(12b) into Eqs.(3b) and (4b), it yields:

$$\tan(h^{S_0}H) = -\frac{\bar{K}^{S_0}}{h^{S_0}H} \quad (13a)$$

$$\tan(h^{S_1}H) = -\frac{\bar{K}^{S_1}}{h^{S_1}H} \quad (13b)$$

where $K^S = k^S + i\omega\delta^S$ is the complex stiffness of viso-elastic supports beneath the pile toe; $\bar{K}^{S_0} = K^S H / E^{S_0}$ and $\bar{K}^{S_1} = K^S H / E^{S_1}$ are the dimensionless coefficient of viso-elastic supports beneath the inner and outer soils, respectively.

Then the eigenvalue $h_n^{S_0}$ and $h_n^{S_1}$ can be further determined by solving Eqs. (13a) and (13b), respectively.

By combining Eqs.(5a), (5b), (13a) and (13b) \tilde{u}^{S_0} and \tilde{u}^{S_1} can be obtained as:

$$\tilde{u}^{S_0} = \sum_{n=1}^{\infty} A_n^{S_0} I_0(q_n^{S_0}r) \cos(h_n^{S_0}z - h_n^{S_0}H) \quad (14a)$$

$$\tilde{u}^{S_1} = \sum_{n=1}^{\infty} A_n^{S_1} K_0(q_n^{S_1}r) \cos(h_n^{S_1}z - h_n^{S_1}H) \quad (14b)$$

where $A_n^{S_0}$ and $A_n^{S_1}$ are undetermined coefficients.

3.2 Vibration of the pipe pile

Due to the non-homogeneous boundary condition at the head of pile, the corresponding general solution for the displacement of pipe pile shaft is rewritten as the following form:

$$\tilde{u}^P(z, r, \omega) = \tilde{u}_1^P(z, r, \omega) + \tilde{u}_2^P(z, \omega) \quad (15)$$

where $\tilde{u}_1^P(z, r, \omega)$ satisfies Eq.(16); $\tilde{u}_2^P(z, \omega)$ satisfies Eqs. (2c), (6a) and (6b).

$$\begin{cases} \nabla^2 \tilde{u}_1^P + \frac{1}{1-2\nu^P} \frac{\partial^2 \tilde{u}_1^P}{\partial z^2} = -\left(\frac{\omega}{V^P}\right)^2 \tilde{u}_1^P \\ G^P \frac{2-2\nu^P}{1-2\nu^P} \frac{\partial \tilde{u}_1^P}{\partial z} \Big|_{z=H} = 0 \\ \frac{\partial \tilde{u}_1^P}{\partial z} + \frac{k^P + i\omega\delta^P}{E^P} \tilde{u}_1^P \Big|_{z=0} = 0 \end{cases} \quad (16)$$

Then, the general solution for Eq.(16) is obtained by:

$$\tilde{u}_1^P = \sum_{n=1}^{\infty} \{A_n^P I_0(q_n^P r) + B_n^P I_0(q_n^P r)\} \cos(h_n^P z - h_n^P H) \quad (17)$$

where A_n^P and B_n^P are undetermined coefficients; $K^P = k^P + i\omega\delta^P$ is the complex stiffness of viso-elastic supports beneath the pile toe; $\bar{K}^P = K^P H / E^P$ denotes the dimensionless coefficient of viso-elastic supports beneath the pile toe; h_n^P can be determined by combining $\tan(h^P H) = -\bar{K}^P / h^P H$, $\bar{K}^P = K^P H / E^P$ and $K^P = k^P + i\omega\delta^P$.

Thus, q_n^P can be further obtained from Eq.(18)

$$(q_n^P)^2 = [(2-2\nu^P)/(1-2\nu^P)](h_n^P)^2 - (\omega/V^P)^2 \quad (18)$$

Substituting $\tilde{u}_2^P(z, \omega)$ into Eq.(2c) yields:

$$\frac{d^2 \tilde{u}_2^P}{dz^2} + (d^P)^2 \tilde{u}_2^P = 0 \quad (19)$$

where $d^P = \frac{\omega}{V^P} \sqrt{(1-2\nu^P)/(2-2\nu^P)}$.

The general solution of Eq. (19) is obtained as:

$$\tilde{u}_2^P(z, \omega) = a^P \cos(d^P z) + b^P \sin(d^P z) \quad (20)$$

where a^P and b^P are undetermined coefficients.

Substituting Eq.(20) into Eqs.(6a) and (6b) yields:

$$a^P = \frac{H\tilde{F}_0(2\nu^P - 1)}{(2-2\nu^P)G^P[\bar{K}^P \cos(d^P H) + d^P H \sin(d^P H)]} \quad (21a)$$

$$b^P = \frac{\bar{K}^P \tilde{F}_0(1-2\nu^P)}{(2-2\nu^P)G^P d^P [\bar{K}^P \cos(d^P H) + d^P H \sin(d^P H)]} \quad (21b)$$

By combining Eqs. (15), (17), (20), (21a) and (21b), the general solution for \tilde{u}^P can be expressed as:

$$\tilde{u}^P(z, r, \omega) = \sum_{n=1}^{\infty} \{A_n^P I_0(q_n^P r) + B_n^P K_0(q_n^P r)\} \cos(h_n^P z - h_n^P H) + \frac{H\tilde{F}_0(2\nu^P - 1)[\cos(d^P z) - \frac{\bar{K}^P}{Hd^P} \sin(d^P z)]}{(2-2\nu^P)G^P[\bar{K}^P \cos(d^P H) + d^P H \sin(d^P H)]} \quad (22)$$

Thus, the shear stress of soils and pile shaft can be expressed as:

$$\tilde{\tau}^{S_0} = \mu^{S_0} \sum_{n=1}^{\infty} q_n^{S_0} A_n^{S_0} I_1(q_n^{S_0} r) \cos(h_n^{S_0} z - h_n^{S_0} H) \quad (23a)$$

$$\tilde{\tau}^{S_1} = -\mu^{S_1} \sum_{n=1}^{\infty} q_n^{S_1} A_n^{S_1} K_1(q_n^{S_1} r) \cos(h_n^{S_1} z - h_n^{S_1} H) \quad (23b)$$

$$\tilde{\tau}^P = G^P \sum_{n=1}^{\infty} q_n^P \{A_n^P I_1(q_n^P r) - B_n^P K_1(q_n^P r)\} \cos(h_n^P z - h_n^P H) \quad (23c)$$

By assuming $\bar{K}^{S_0} = \bar{K}^{S_1} = \bar{K}^P$, it gives $h_n^{S_0} = h_n^{S_1} = h_n^P = h_n$.

Inserting Eqs.(14a) and (22) into (7a), and substituting Eqs.(14b) and (22) into (7b), respectively, the following expressions can be obtained

$$\begin{aligned} & \sum_{n=1}^{\infty} A_n^{S_0} I_0(q_n^{S_0} r_0) \cos(h_n z - h_n H) \\ &= \sum_{n=1}^{\infty} \{A_n^P I_0(q_n^P r_0) + B_n^P K_0(q_n^P r_0)\} \cos(h_n z - h_n H) + \frac{H\tilde{F}_0(2\nu^P - 1)[\cos(d^P z) - \frac{\bar{K}^P}{Hd^P} \sin(d^P z)]}{(2 - 2\nu^P)G^P[\bar{K}^P \cos(d^P H) + d^P H \sin(d^P H)]} \end{aligned} \quad (24a)$$

$$\begin{aligned} & \sum_{n=1}^{\infty} A_n^{S_1} K_0(q_n^{S_1} r_1) \cos(h_n z - h_n H) \\ &= \sum_{n=1}^{\infty} \{A_n^P I_0(q_n^P r_1) + B_n^P K_0(q_n^P r_1)\} \cos(h_n z - h_n H) + \frac{H\tilde{F}_0(2\nu^P - 1)[\cos(d^P z) - \frac{\bar{K}^P}{Hd^P} \sin(d^P z)]}{(2 - 2\nu^P)G^P[\bar{K}^P \cos(d^P H) + d^P H \sin(d^P H)]} \end{aligned} \quad (24b)$$

Inserting Eqs.(23a) and (23c) into (7c) and substituting Eqs.(23b) and (23c) into (7d), respectively, we have

$$\mu^{S_0} q_n^{S_0} A_n^{S_0} I_1(q_n^{S_0} r_0) = G^P q_n^P \{A_n^P I_1(q_n^P r_0) - B_n^P K_1(q_n^P r_0)\} \quad (25a)$$

$$-\mu^{S_1} q_n^{S_1} A_n^{S_1} K_1(q_n^{S_1} r_1) = G^P q_n^P \{A_n^P I_1(q_n^P r_1) - B_n^P K_1(q_n^P r_1)\} \quad (25b)$$

Thus, multiplying both sides of Eqs.(24a) and (24b) by $\cos(h_n z - h_n H)$ and integrating it between the limits $[0, H]$, respectively, it produces

$$L_n A_n^{S_0} I_0(q_n^{S_0} r_0) = L_n \{A_n^P I_0(q_n^P r_0) + B_n^P K_0(q_n^P r_0)\} + \frac{H\tilde{F}_0(2\nu^P - 1)}{(2 - 2\nu^P)G^P} \phi_n \quad (26a)$$

$$L_n A_n^{S_1} K_0(q_n^{S_1} r_1) = L_n \{A_n^P I_0(q_n^P r_1) + B_n^P K_0(q_n^P r_1)\} + \frac{H\tilde{F}_0(2\nu^P - 1)}{(2 - 2\nu^P)G^P} \phi_n \quad (26b)$$

where $L_n = \int_0^H \cos^2(h_n z - h_n H) dz$, $\phi_n = \int_0^H \frac{\cos(d^P z) - \sin(d^P z) \bar{K}^P / Hd^P}{\bar{K}^P \cos(d^P H) + d^P H \sin(d^P H)} \cos(h_n z - h_n H) dz$.

By combining Eqs.(25a), (25b), (26a) and (26b), the corresponding undetermined coefficients A_n^P and B_n^P can be determined as

$$A_n^P = \frac{\alpha_{11} - \alpha_{21}}{\alpha_{11}\alpha_{22} - \alpha_{12}\alpha_{21}} \frac{H\tilde{F}_0(2\nu^P - 1)}{(2 - 2\nu^P)G^P} \phi_n \quad (27a)$$

$$B_n^P = \frac{\alpha_{22} - \alpha_{12}}{\alpha_{11}\alpha_{22} - \alpha_{12}\alpha_{21}} \frac{H\tilde{F}_0(2\nu^P - 1)}{(2 - 2\nu^P)G^P} \phi_n \quad (27b)$$

1
2
3
4
5
6
7
8
9

$$\text{where } \alpha_{11} = \frac{L_n G^P q_n^P K_1(q_n^P r_1) K_0(q_n^{S_1} r_1)}{\mu^{S_1} q_n^{S_1} K_1(q_n^{S_1} r_1)} - L_n K_0(q_n^P r_1), \alpha_{12} = -\frac{L_n G^P q_n^P I_1(q_n^P r_1) K_0(q_n^{S_1} r_1)}{\mu^{S_1} q_n^{S_1} K_1(q_n^{S_1} r_1)} - L_n I_0(q_n^P r_1)$$

$$\alpha_{21} = -\frac{L_n G^P q_n^P I_0(q_n^{S_0} r_0) K_1(q_n^P r_0)}{\mu^{S_0} q_n^{S_0} I_1(q_n^{S_0} r_0)} - L_n K_0(q_n^P r_0), \alpha_{22} = \frac{L_n G^P q_n^P I_0(q_n^{S_0} r_0) I_1(q_n^P r_0)}{\mu^{S_0} q_n^{S_0} I_1(q_n^{S_0} r_0)} - L_n I_0(q_n^P r_0).$$

10
11
12
13
14
15
16
17
18
19

Therefore, the longitudinal displacement function of pipe pile in frequency domain can be expressed by

$$\tilde{u}^P(z, r, \omega) = \frac{H \tilde{F}_0 (2v^P - 1)}{(2 - 2v^P) G^P} \left\{ \sum_{n=1}^{\infty} \frac{(\alpha_{11} - \alpha_{21}) I_0(q_n^P r) + (\alpha_{22} - \alpha_{12}) K_0(q_n^P r)}{\alpha_{11} \alpha_{22} - \alpha_{12} \alpha_{21}} \phi_n \cos(h_n^P z - h_n^P H) + \frac{\cos(d^P z) - (\bar{K}^P / H d^P) \sin(d^P z)}{\bar{K}^P \cos(d^P H) + d^P H \sin(d^P H)} \right\} \quad (28)$$

20
21
22
23
24
25
26
27
28
29

Furthermore, the frequency response function for the longitudinal displacement can be written as:

$$H_u(r, \omega) = \frac{\tilde{u}^P|_{z=H}}{\tilde{F}_0} = \frac{H(2v^P - 1)}{(2 - 2v^P) G^P} \left\{ \sum_{n=1}^{\infty} \frac{(\alpha_{11} - \alpha_{21}) I_0(q_n^P r)}{\alpha_{11} \alpha_{22} - \alpha_{12} \alpha_{21}} + \frac{(\alpha_{22} - \alpha_{12}) K_0(q_n^P r)}{\alpha_{11} \alpha_{22} - \alpha_{12} \alpha_{21}} \phi_n + \frac{\cos(d^P H) - (\bar{K}^P / H d^P) \sin(d^P H)}{\bar{K}^P \cos(d^P H) + d^P H \sin(d^P H)} \right\} \quad (29)$$

30
31
32
33
34
35
36
37
38
39

The longitudinal complex impedance function for the pile head $K_d(r, \omega)$ is given as:

$$K_d(r, \omega) = \frac{1}{H_u(r, \omega)} = K_r(r, \omega) + iK_i(r, \omega) \quad (30)$$

40
41
42
43
44
45
46
47
48
49

where $K_r(r, \omega)$ and $K_i(r, \omega)$ are the dynamic stiffness and damping, respectively.

50
51
52
53
54
55
56
57
58
59

For the convenience to perform further comparative analysis, with respect to the previous solutions which are derived from the Euler–Bernoulli model and the Rayleigh–Love model, the cross-sectional equivalent frequency response function of longitudinal displacement for pile head is defined by

$$\bar{H}_u(\omega) = \frac{1}{\pi(r_1^2 - r_0^2)} \int_0^{2\pi} \int_{r_0}^{r_1} H_u(r, \omega) r dr d\varphi$$

$$= \frac{H(2v^P - 1)}{(2 - 2v^P) G^P} \left\{ \sum_{n=1}^{\infty} \frac{2\phi_n (\alpha_{11} - \alpha_{21}) [r_1 I_1(q_n^P r_1) - r_0 I_1(q_n^P r_0)]}{q_n^P (\alpha_{11} \alpha_{22} - \alpha_{12} \alpha_{21}) (r_1^2 - r_0^2)} + \frac{\cos(d^P H) - (\bar{K}^P / H d^P) \sin(d^P H)}{\bar{K}^P \cos(d^P H) + d^P H \sin(d^P H)} \right\} \quad (31)$$

60
61
62
63
64
65

Thus, the cross-sectional equivalent complex impedance for pile head can be easily defined by

$$\bar{K}_d(\omega) = \frac{1}{\bar{H}_u(\omega)} = \bar{K}_r(\omega) + i\bar{K}_i(\omega) \quad (32)$$

where $\bar{K}_r(\omega)$ and $\bar{K}_i(\omega)$ denote the cross-sectional equivalent dynamic stiffness and damping, respectively.

4. Results and discussions

In this section, numerical examples are illustrated to validate the obtained analytical

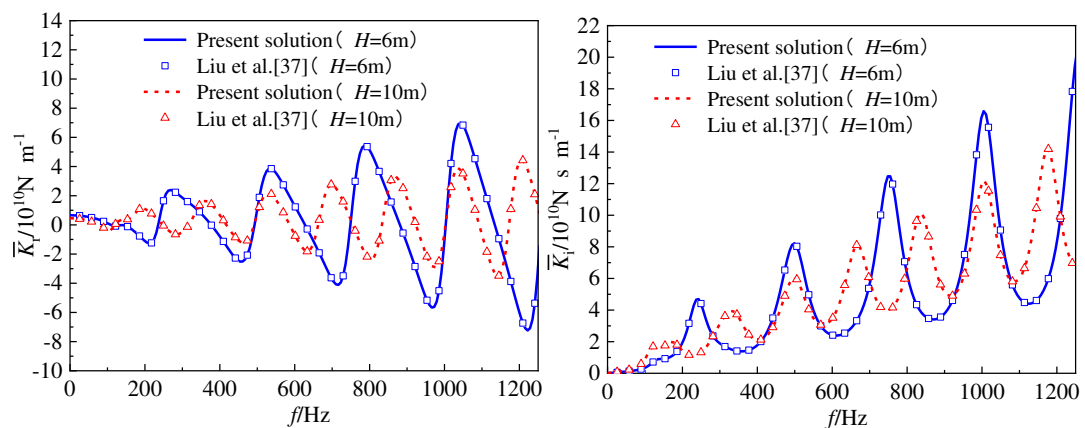
solutions via comparisons with previous solutions. Comparative analyses are also performed to illustrate the difference between the present and previous solutions, concerning the wave propagation effect in radial direction on the longitudinal dynamic characteristics of pile shaft. Furthermore, the effects of Poisson ratio and visco-elastic support beneath the pile toe, on the longitudinal dynamic characteristics of pile shaft, are investigated. Unless other specified, the mechanical parameters are used as follows:

$$H = 6\text{m} ; E^P = 40\text{GPa} ; \rho^P = 2500\text{kg m}^{-3} ; \nu^P = 0.35 ; r_0 = 0.3\text{m} ; r_1 = 0.6\text{m} ; \nu^{S_1} = \nu^{S_0} = 0.35 ; \xi^{S_1} = \xi^{S_0} = 0.02 ; G^{S_1} = G^{S_0} = 20\text{MPa} ; \rho^{S_1} = \rho^{S_0} = 2000\text{kg m}^{-3} ; \bar{K}^{S_0} = \bar{K}^{S_1} = \bar{K}^P = 1.0 .$$

4.1 Verification of the proposed solution

The cross-sectional equivalent complex impedance written in Eq.(32) can be reduced to depict the longitudinal vibration of a pipe pile with fixed end supports by setting $\bar{K}^{S_0} = \bar{K}^{S_1} = \bar{K}^P \rightarrow \infty$. Thus, the proposed solution can be validated by comparing it with the solution of Liu et al. [37] in the same parameter system. As can be seen from Fig. 2, the proposed solution for the cross-sectional equivalent complex impedance with different pile length H is in great agreement with that derived by Liu et al. [37]. Similarly, the proposed solution is also reduced to compare with the existing solution of Meng et al. [48] by setting $r_0 \rightarrow 0$, as shown in Fig.3. It is observed that the proposed solution for the cross-sectional equivalent complex impedance with different pile length H also agrees well with the previous solution of Meng et al. [48]. Hence, the validity of the proposed solution can be verified with the above independent comparisons.

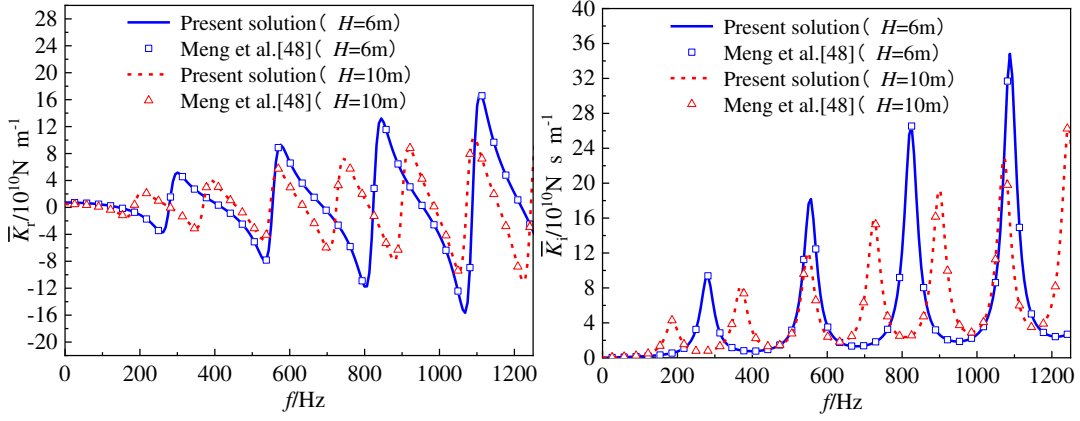
As the proposed solution is, the existing solutions above are also derived from the wave propagation theory of 3D continuum for the whole pile-soil system. It is noted that the further consideration of the visco-elastic supports beneath pile toe (3D-continuum pile model) leads to total differences in the vibration mode, eigenfunctions for displacement and orthogonality of eigenfunctions, from those of the solution derived by Liu et al [37].



(a) Cross-sectional equivalent dynamic stiffness (b) Cross-sectional equivalent dynamic damping

Fig. 2 Comparison of the cross-sectional equivalent complex impedance in reduced form

($\bar{K}^{S_0} = \bar{K}^{S_1} = \bar{K}^P \rightarrow \infty$) with the solution of Liu et al. [37]



(a) Cross-sectional equivalent dynamic stiffness (b) Cross-sectional equivalent dynamic damping

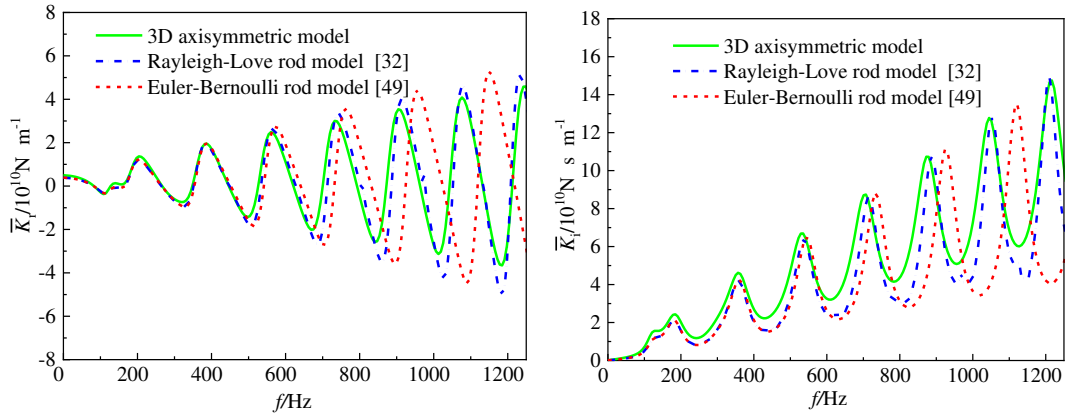
Fig. 3 Comparison of the cross-sectional equivalent complex impedance in reduced form

($r_0 \rightarrow 0$) with the solution of Meng et al. [48]

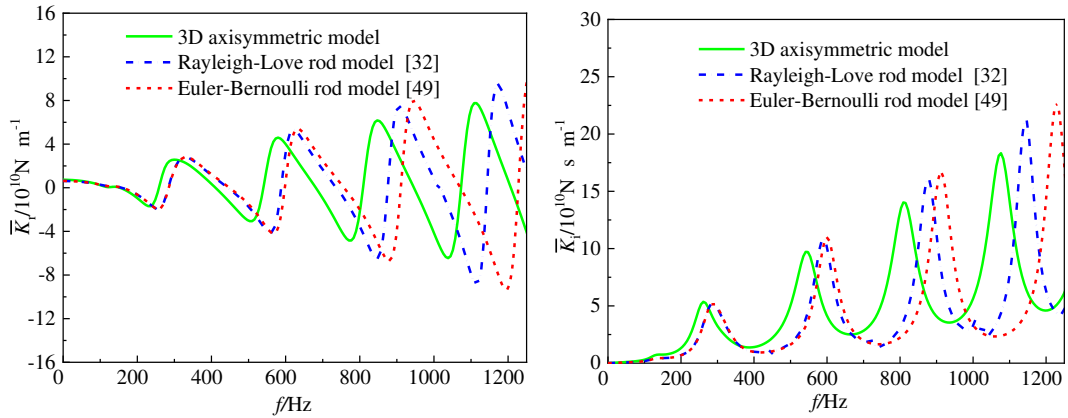
4.2 Comparative analyses of the proposed solution

As for the Euler–Bernoulli rod model, the wave propagation effect of pile shaft in radial direction is completely ignored. Approximately, the Rayleigh–Love model takes this radial wave effect into account by introducing Poisson’s ratio to the governing equation. For the aim to demonstrate the difference, between the present solution and previous solutions derived from rod-type models of pile shaft, i.e., the Rayleigh–Love [32] and Euler–Bernoulli [49] rod models, comparative analyses are performed.

Fig.4 and Fig.5 depict the difference between the present and previous solutions with $H=12\text{m}$ ($H/r_1 = 20$) and $H=6\text{m}$ ($H/r_1 = 10$), respectively. Since the present solution considers the 3D wave propagation effect within the pile shaft, it is clear that the resonance frequency and amplitude of complex impedance are both smaller than those corresponding to the Rayleigh–Love and *Euler–Bernoulli rod models*, and this difference becomes more obvious as the frequency increases. Furthermore, the solution from the Rayleigh–Love rod model is closer to the present solution than that from *the Euler–Bernoulli rod model*. With the decrease of pile slenderness ratio (i.e., to keep the cross-section of pile constant and decrease the pile length from $H=12\text{m}$ to $H=6\text{m}$), the difference between the present and previous solutions gets greater, especially within high-frequency range. It indicates that, even though the Rayleigh–Love rod model can roughly consider the radial wave effect on pile vibration in certain circumstances, it may lead to an overestimation of the pile’s complex impedance, especially for piles with small slenderness ratio or high-frequency excitation.



(a) Cross-sectional equivalent dynamic stiffness (b) Cross-sectional equivalent dynamic damping
 Fig. 4 Comparison of the cross-sectional equivalent complex impedance obtained from different models ($H=12\text{m}$, $H/r_1 = 20$)



(a) Cross-sectional equivalent dynamic stiffness (b) Cross-sectional equivalent dynamic damping
 Fig. 5 Comparison of the cross-sectional equivalent complex impedance obtained from different models ($H=6\text{m}$, $H/r_1 = 10$)

Fig.6 illustrates some typical points (i.e., P1, P2, and P3) at the pile head. As shown in Fig.7, a comparison of the complex impedance solution at the typical points is performed. It should be noted that a frequency interval (from 1078 to 1124 Hz) adjacent to the fourth resonance frequency is specified for the convenience to examine the radial wave effect on the complex impedance of pile head. It can be found that the fourth resonance frequencies corresponding to dynamic stiffness and dynamic damping are 1,116 Hz and 1,080 Hz, respectively. In addition, substituting the fourth resonance frequency of dynamic stiffness and damping into Eq. (30), it yields the cross-sectional contours of the complex impedance of pile head as shown in Fig.8. It can be seen from Fig.7 and Fig.8, that there exists a significant annular variance of complex impedance along the radial direction of the pile head. Specifically, the dynamic stiffness increases first and decreases afterward, while the dynamic damping keeps increasing, with the change of corresponding position from the inner to the outer of the pile head.

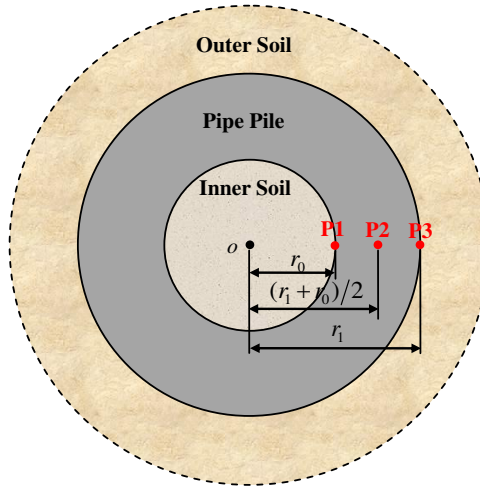


Fig. 6 Typical points at the pile head

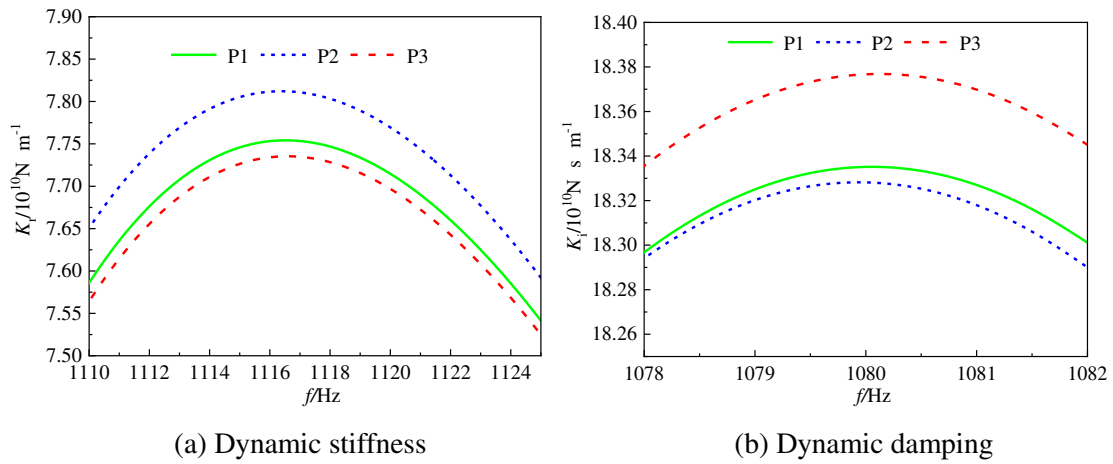
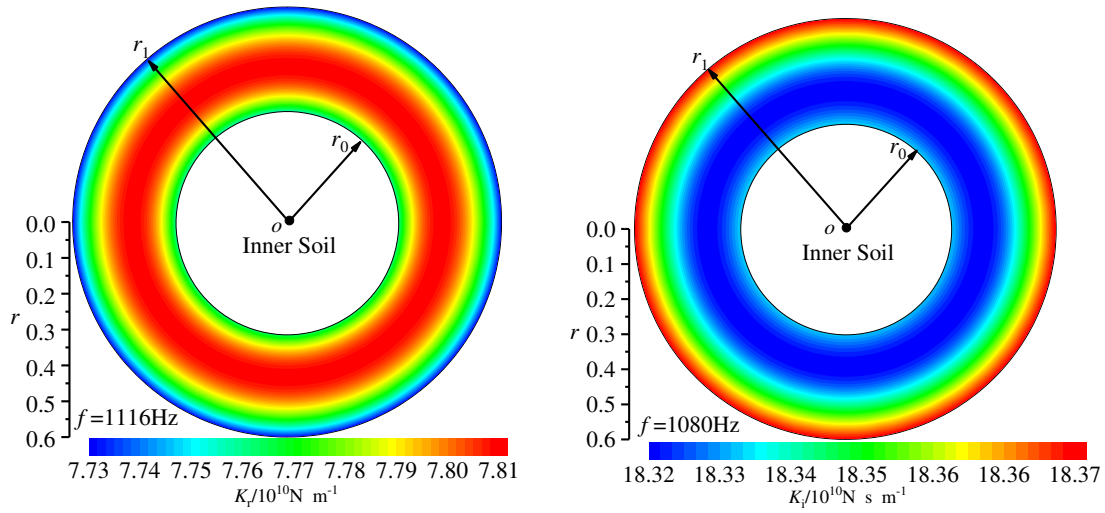


Fig. 7 Comparison of the complex impedance at the typical points of pile head

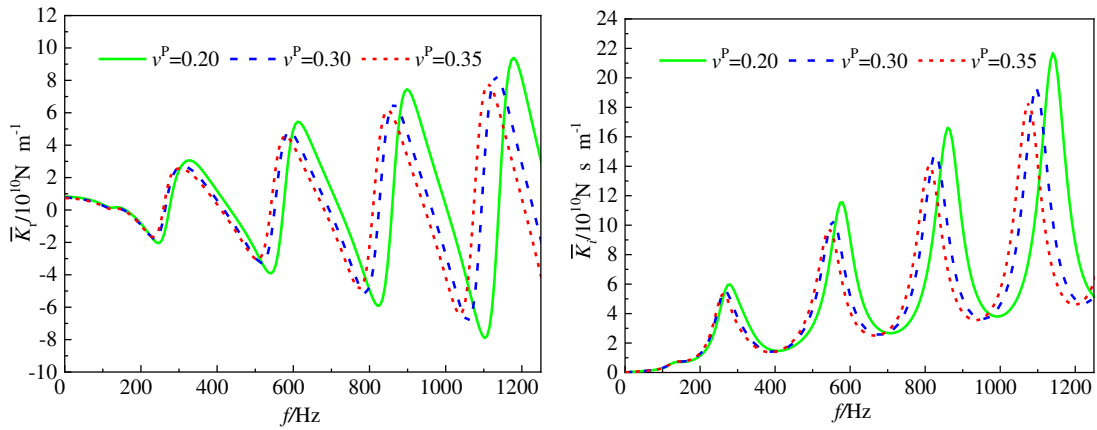
The effect of Poisson's ratio on the cross-sectional equivalent complex impedance for pile head is shown in Fig. 9. It can be observed that both the resonance amplitude and frequency of complex impedance decrease with the rise of Poisson's ratio. As the frequency increases, this tendency becomes more obvious. Fig. 10 shows that the dimensionless coefficient of visco-elastic support beneath the pile toe has a considerable effect on the phase of the cross-sectional equivalent complex impedance for pile head. To be specific, the resonance frequency of complex impedance decreases as the dimensionless coefficient of visco-elastic supports increases, while the effect on the resonance amplitude can be ignored.



(a) Dynamic stiffness

(b) Dynamic damping

Fig.8 Cross-sectional contours of the complex impedance for pile head

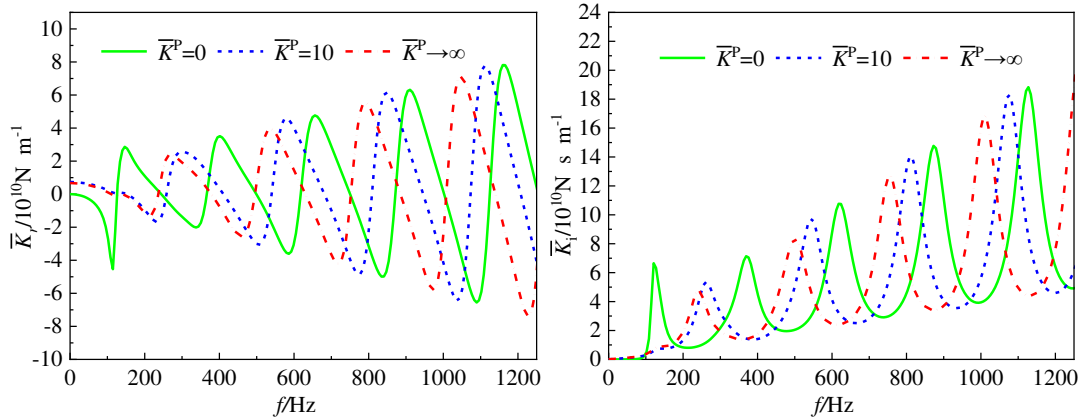


(a) Cross-sectional equivalent dynamic stiffness

(b) Cross-sectional equivalent dynamic damping

Fig. 9 Effect of Poisson's ratio on the cross-sectional equivalent complex impedance for pile

head



(a) Cross-sectional equivalent dynamic stiffness

(b) Cross-sectional equivalent dynamic damping

Fig.10 Effect of the supports beneath the pile toe on the cross-sectional equivalent complex

impedance for pile head

5. Conclusions

A novel approach is presented to describe the longitudinal vibration system of a large-diameter floating pipe pile and surrounding soils based on the wave propagation theory of 3D continuum. The corresponding analytical solutions for longitudinal complex impedance are obtained and subsequently verified by comparisons with existing solutions. Comparative analyses are also performed to discuss the difference between the present and previous solutions, which reveals the wave propagation effect in radial direction on the longitudinal dynamic vibration of pile shaft. Furthermore, the effects of Poisson ratio and visco-elastic support beneath the pile toe, on the longitudinal dynamic vibration of pile shaft, are examined. The results indicate that:

(1) The resonance frequency and amplitude of the present solution are both smaller than those corresponding to the Rayleigh–Love and *Euler–Bernoulli rod models*, and this difference becomes more obvious as the frequency increases.

(2) Even though the Rayleigh–Love rod model can approximately consider the radial wave effect on pile vibration in certain circumstances, it may lead to an overestimation of the pile's complex impedance, especially for piles with small slenderness ratio or high-frequency excitation.

(3) Both the resonance amplitude and frequency of complex impedance decline with the rise of Poisson's ratio. Differently, the resonance frequency of complex impedance decreases as the dimensionless coefficient of visco-elastic supports increases, while the effect on the resonance amplitude can be ignored.

(4) The proposed approach and corresponding solutions provide a more extensive scope of application for longitudinal vibration analysis of a large-diameter floating pipe pile, which can also be reduced to analyze the longitudinal vibration problems of large-diameter floating solid pile and fixed- end pipe pile.

Acknowledgments

This work is supported by the National Natural Science Foundation of China (Grant No. 51878109, 51778107 and 51578100), the Fundamental Research Funds for the Central Universities (Grant No. 3132019601), and China Scholarship Council (CSC No.201806570004). The corresponding author would like to acknowledge the support from State Key Laboratory of Coastal and Offshore Engineering, Dalian University of Technology.

References

- [1] R. Varghese, A. Boominathan, S. Banerjee, *Stiffness and load sharing characteristics of piled raft foundations*

- subjected to dynamic loads, *Soil Dyn. Earthq. Eng.* 133(2020) 106177.
<https://doi.org/10.1016/j.soildyn.2020.106117>
- [2] Y. Xu, Z. Zeng, Z. Wang, H. Yan, Seismic study of a widened and reconstructed long-span continuous steel truss bridge, *Struct. Infrastruct. E.* 2020. <https://doi.org/10.1080/15732479.2020.1733621>
- [3] L. Gao, K. H. Wang, S. Xiao, Z. Y. Li, J. T. Wu, An analytical solution for excited pile vibrations with variable section impedance in the time domain and its engineering application, *Comput. Geotech.* 73(2016) 170-178. <https://doi.org/10.1016/j.compgeo.2015.12.008>
- [4] M. Allani, A. Holeyman, Numerical evaluation of effects of nonlinear lateral pile vibrations on nonlinear axial response of pile shaft, *Soils Found.* 53(2013) 395-407. <https://doi.org/10.1016/j.sandf.2013.04.002>
- [5] S. Carbonari, M. Morici, F. Dezi, G. Leoni, Analytical evaluation of impedances and kinematic response of inclined piles, *Eng. Struct.* 117(2016) 384-396. <https://doi.org/10.1016/j.engstruct.2016.03.027>
- [6] C. Y. Cui, K. Meng, Y. J. Wu, D. Chapman, Z. M. Liang, Dynamic response of pipe pile embedded in layered visco-elastic media with radial inhomogeneity under vertical excitation, *Geomech. Eng.* 16(2018) 609-618. <https://doi.org/10.12989/gae.2018.16.6.609>
- [7] T. G. Davies, M. Budhu, Nonlinear analysis of laterally loaded piles in heavily overconsolidated clays, *Geotechnique* 36(1986) 527-538. <http://dx.doi.org/10.1680/geot.1986.36.4.527>
- [8] S. Dash, S. Bhattacharya, A. Blakeborough, Bending-buckling interaction as a failure mechanism of piles in liquefiable soils, *Soil Dyn. Earthq. Eng.* 30(2010) 32-39. <https://doi.org/10.1016/j.soildyn.2009.08.002>
- [9] M. Elkasabgy, M. H. El Nagggar, Dynamic response of vertically loaded helical and driven steel piles, *Can. Geotech. J.* 50(2013) 521-535. <https://doi.org/10.1139/cgj-2011-0126>
- [10] R. Dobry, G. Gazetas, Simple method for dynamic stiffness and damping of floating pile groups, *Geotechnique* 38(1988) 557-574. <http://dx.doi.org/10.1680/geot.1988.38.4.557>
- [11] K. H. Wang, W. B. Wu, Z. Q. Zhang, C. J. Leo, Vertical dynamic response of an inhomogeneous viscoelastic pile, *Comput. Geotech.* 37(2010), 536-544. <https://doi.org/10.1016/j.compgeo.2010.03.001>
- [12] M. Shadlou, S. Bhattacharya, Dynamic stiffness of pile in a layered continuum, *Géotechnique* 64(2014) 303-319. <https://doi.org/10.1680/geot.13.P.107>
- [13] T. Nogami, K. Konagai, Dynamic Response of Vertically Loaded Nonlinear Pile Foundations, *J. Geotech. Eng.* 113(1987) 147-160. [https://doi.org/10.1061/\(ASCE\)0733-9410\(1987\)113:2\(147\)](https://doi.org/10.1061/(ASCE)0733-9410(1987)113:2(147))
- [14] Y. Han, H. Vaziri, Dynamic response of pile groups under lateral loading, *Soil. Dyn. Earthq. Eng.* 11 (1992) 87-99. [https://doi.org/10.1016/0267-7261\(92\)90047-H](https://doi.org/10.1016/0267-7261(92)90047-H)
- [15] G. Anoyatis, G. Mylonakis, Dynamic Winkler modulus for axially loaded piles, *Geotechnique* 62(2012) 521-536. <https://doi.org/10.1680/geot.11.P.052>
- [16] M. Novak, Dynamic Stiffness and Damping of Piles, *Can. Geotech. J.* 11(1974) 574-598. <https://doi.org/10.1139/t74-059>
- [17] G. Mylonakis, Winkler modulus for axially loaded piles, *Geotechnique* 51(2001) 455-461. <https://doi.org/10.1680/geot.2001.51.5.455>
- [18] T. Nogami, M. Novák, Soil-pile interaction in vertical vibration, *Earthq. Eng. Struct. D.* 4(1976) 277-293. <https://doi.org/10.1002/eqe.4290040308>
- [19] C. B. Hu, K. H. Wang, K. H. Xie, Time domain axial response of dynamically loaded pile in viscous damping soil layer, *J. Vib. Eng.* 17(2004), 72-77. <https://doi.org/10.3969/j.issn.1004-4523.2004.01.016>
- [20] W. B. Wu, K. H. Wang, Z. Q. Zhang, C. J. Leo, Soil- pile interaction in the pile vertical vibration considering true three- dimensional wave effect of soil, *Int. J. Numer. Anal. Met.* 37(2013) 2860-2876. <https://doi.org/10.1002/nag.2164>
- [21] M. H. El Nagggar, M. Novak, Nonlinear axial interaction in pile dynamics, *J. Geotech. Eng.* 120(1994) 678-695. [https://doi.org/10.1061/\(ASCE\)0733-9410\(1994\)120:4\(678\)](https://doi.org/10.1061/(ASCE)0733-9410(1994)120:4(678))

- 1
2
3
4
5
6
7
8
9
10
11
12
13
14
15
16
17
18
19
20
21
22
23
24
25
26
27
28
29
30
31
32
33
34
35
36
37
38
39
40
41
42
43
44
45
46
47
48
49
50
51
52
53
54
55
56
57
58
59
60
61
62
63
64
65
- [22] M. Hesham, M. H. El Naggar, Vertical and torsional soil reactions for radially inhomogeneous soil layer, *Struct. Eng. Mech.* 10(2000) 299-312. <https://doi.org/10.12989/sem.2000.10.4.299>
- [23] K. H. Wang, D. Y. Yang, Z. Q. Zhang, C. J. Leo, A new approach for vertical impedance in radially inhomogeneous soil layer, *Int. J. Numer. Anal. Met.* 36(2012) 697-707. <https://doi.org/10.1002/nag.1024>
- [24] Z. Li, Y. Gong, Discussion on three dimensional effect of wave propagating in the pile with large diameter, *Chin. J. Rock Mech. Eng.* 17(1998) 434-439.
- [25] Y.K. Chow, K. K. Phoon, W. F. Chow, Low strain integrity testing of piles: 3D effects. *J. Geotechn. Geoenviron. Eng.* 129(2003) 1057-1062. [https://doi.org/10.1061/\(ASCE\)1090-0241\(2003\)129:11\(1057\)](https://doi.org/10.1061/(ASCE)1090-0241(2003)129:11(1057))
- [26] M. Krawczuk, J. Grabowska, M. Palacz, Longitudinal wave propagation. Part I-Comparison of rod theories, *J. Sound Vib.* 295(2006) 461-478. <https://doi.org/10.1016/j.jsv.2005.12.048>
- [27] H. Y. Chai, K. K. Phoon, D. J. Zhang, Effects of the source on wave propagation in pile integrity testing, *J. Geotech. Geoenviron. Eng.* 136(2010) 1200-1208. [https://doi.org/10.1061/\(ASCE\)GT.1943-5606.0000272](https://doi.org/10.1061/(ASCE)GT.1943-5606.0000272)
- [28] W. B. Wu, G. S. Jiang, B. Dou, C. J. Leo, Vertical dynamic impedance of tapered pile considering compacting effect, *Math. Probl. Eng.* 2013 1-9. <https://doi.org/10.1155/2013/304856>
- [29] S. H. Lu, K. H. Wang, W. B. Wu, C. J. Leo, Longitudinal vibration of pile in layered soil based on Rayleigh-Love rod theory and fictitious soil-pile model, *J. Cent. South Uni.* 22(2015) 1909-1918. <https://doi.org/10.1007/s11771-015-2710-8>
- [30] S. H. Lu, K. H. Wang, W. B. Wu, C. J. Leo, Longitudinal vibration of a pile embedded in layered soil considering the transverse inertia effect of pile, *Comput. Geotech.* 62(2014) 90-99. <https://doi.org/10.1016/j.compgeo.2014.06.015>
- [31] Z. Y. Li, K. H. Wang, W. B. Wu, C. J. Leo, Vertical vibration of a large diameter pile embedded in inhomogeneous soil based on the Rayleigh-Love rod theory, *J. Zhejiang Uni. Sci. A* 17(2016) 974-988. <https://doi.org/10.1631/jzus.a1500341>
- [32] C. J. Zheng, H. L. Liu, X. M. Ding, H. Zhou, Vertical vibration of a large diameter pipe pile considering transverse inertia effect of pile, *J. Cent. South Uni.* 23(2016) 891-897. <https://doi.org/10.1007/s11771-016-3136-7>
- [33] Z. Y. Li, K. H. Wang, W. B. Wu, C. J. Leo, N. Wang, Vertical vibration of a large-diameter pipe pile considering the radial inhomogeneity of soil caused by the construction disturbance effect, *Comput. Geotech.* 85(2017) 90-102. <https://doi.org/10.1016/j.compgeo.2016.12.016>
- [34] K. Fei, H. L. Liu, T. Zhang, Three-dimensional effects in low strain integrity test of PCC pile, *Rock Soil Mechan.* 28(2007) 1095-1102. <https://doi.org/10.3969/j.issn.1000-7598.2007.06.006>
- [35] H. L. Liu, X. M. Ding, Analytical solution of dynamic response of cast-in-situ concrete thin-wall pipe piles under transient concentrated load with low strain, *Chin. J. Rock Mech. Eng.* 29(2007) 1611-1617. <https://doi.org/10.3321/j.issn:1000-4548.2007.11.003>
- [36] X. M. Ding, H. L. Liu, B. Zhang, High-frequency interference in low strain integrity testing of large-diameter pipe piles, *Sci. China Technol. Sci.* 54(2011) 420-430. <https://doi.org/10.1007/s11431-010-4235-6>
- [37] L. C. Liu, Q. F. Yan, S. WANG, Q. Q. Chen, Vertical vibration of pipe pile based on axisymmetric model, *Rock Soil Mechan.* 37(2016) 119-125.
- [38] C. J. Zheng, H. L. Liu, G. P. Kouretzis, S. W. Sloan, X. M. Ding, Vertical response of a thin-walled pipe pile embedded in viscoelastic soil to a transient point load with application to low-strain integrity testing, *Comput. Geotech.* 70 (2015) 50-59. <https://doi.org/10.1016/j.compgeo.2015.07.016>
- [39] W. B. Wu, K. H. Wang, Z. Q. Zhang, C. J. Leo, Soil-pile interaction in the pile vertical vibration considering true three-dimensional wave effect of soil, *Int. J. Numer. Anal. Met.* 37(2013), 2860-2876. <https://dx.doi.org/10.1002/nag.2164>

- 1
2
3
4
5
6
7
8
9
10
11
12
13
14
15
16
17
18
19
20
21
22
23
24
25
26
27
28
29
30
31
32
33
34
35
36
37
38
39
40
41
42
43
44
45
46
47
48
49
50
51
52
53
54
55
56
57
58
59
60
61
62
63
64
65
- [40] H. L. Liu, C. J. Zheng, X. M. Ding, H. Qin, Vertical dynamic response of a pipe pile in saturated soil layer, *Comput. Geotech.* 61(2014), 57-66. <https://dx.doi.org/10.1016/j.compgeo.2014.04.006>
- [41] T. Senjuntichai, S. Keawsawasvong, R. K. N. D. Rajapakse, Vertical vibration of a circular foundation in a transversely isotropic poroelastic soil, *Comput. Geotech.* 122(2020), 103550. <https://dx.doi.org/10.1016/j.compgeo.2020.103550>
- [42] L. Gao, K. H. Wang, J. Wu, S. Xiao, N. Wang, Analytical solution for the dynamic response of a pile with a variable-section interface in low-strain integrity testing, *J Sound. Vib.* 395(2017) 328-340. <https://dx.doi.org/10.1016/j.jsv.2017.02.037>
- [43] B. Manna, D. K. Baidya, Dynamic nonlinear response of pile foundations under vertical vibration-theory versus experiment, *Soil Dyn. Earthq. Eng.* 30(2010), 456-469. <https://dx.doi.org/10.1016/j.soildyn.2010.01.002>
- [44] M. Zhou, H. Liu, M. S. Hossain, Y. Hu, T. Zhang, Numerical simulation of plug formation during casing installation of cast-in-place concrete pipe (PCC) piles, *Can. Geotech. J.* 53(2016), 1093-1109. <https://dx.doi.org/10.1139/cgj-2015-0162>
- [45] C. Zheng, H. Liu, X. Ding, G. P. Kouretzis, D. Sheng, Three-dimensional effects in low-strain integrity testing of large diameter pipe piles, *J.Eng. Mech.* 142(2016), 04016064. [https://dx.doi.org/10.1061/\(ASCE\)EM.1943-7889.0001117](https://dx.doi.org/10.1061/(ASCE)EM.1943-7889.0001117)
- [46] C. Zheng, H. Liu, X. Ding, G. P. Kouretzis, Resistance of inner soil to the vertical vibration of pipe piles, *Soil Dyn. Earthq. Eng.* 94(2017), 83-87. <https://dx.doi.org/10.1016/j.soildyn.2017.01.002>
- [47] X. Ding, H. Liu, G. Kong, C. Zheng, Time-domain analysis of velocity waves in a pipe pile due to a transient point load, *Comput. Geotech.* 58(2014), 101-116. <https://dx.doi.org/10.1016/j.compgeo.2014.02.004>
- [48] K. Meng, C. Y. Cui, C. S. Xu, Z. M. Liang, Z. G. Sun, B. L. Wang, Vertical dynamic impedance of floating pile considering the radial wave effect, *J.Vib. Eng.* 32(2019) 296-304.
- [49] C. J. Zheng, X. M. Ding, Y. F. Sun, Vertical vibration of a pipe pile in viscoelastic soil considering the three-dimensional wave effect of soil, *Int. J. Geomech.* 16(2016) 04015037. [https://doi.org/10.1061/\(asce\)gm.1943-5622.0000529](https://doi.org/10.1061/(asce)gm.1943-5622.0000529)

Declaration of interests

The authors declare that they have no known competing financial interests or personal relationships that could have appeared to influence the work reported in this paper.

The authors declare the following financial interests/personal relationships which may be considered as potential competing interests:

Fig.1

[Click here to download high resolution image](#)

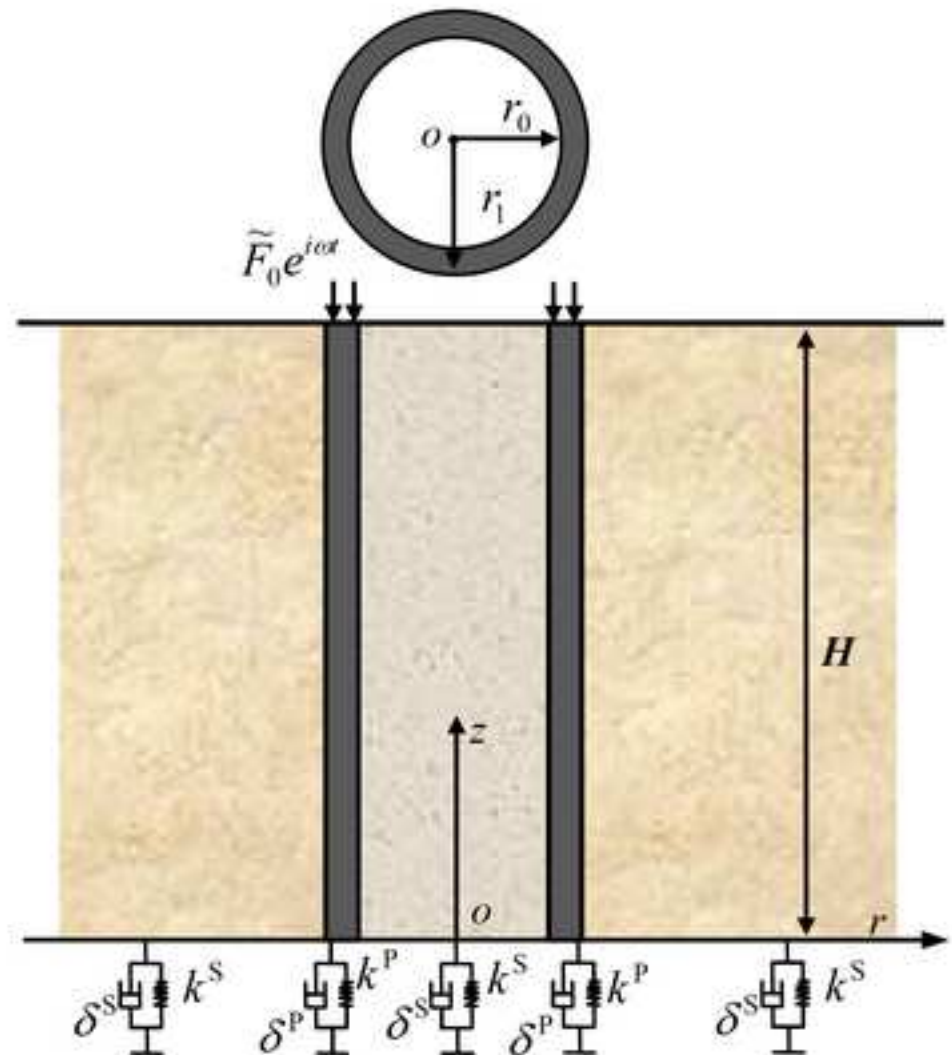
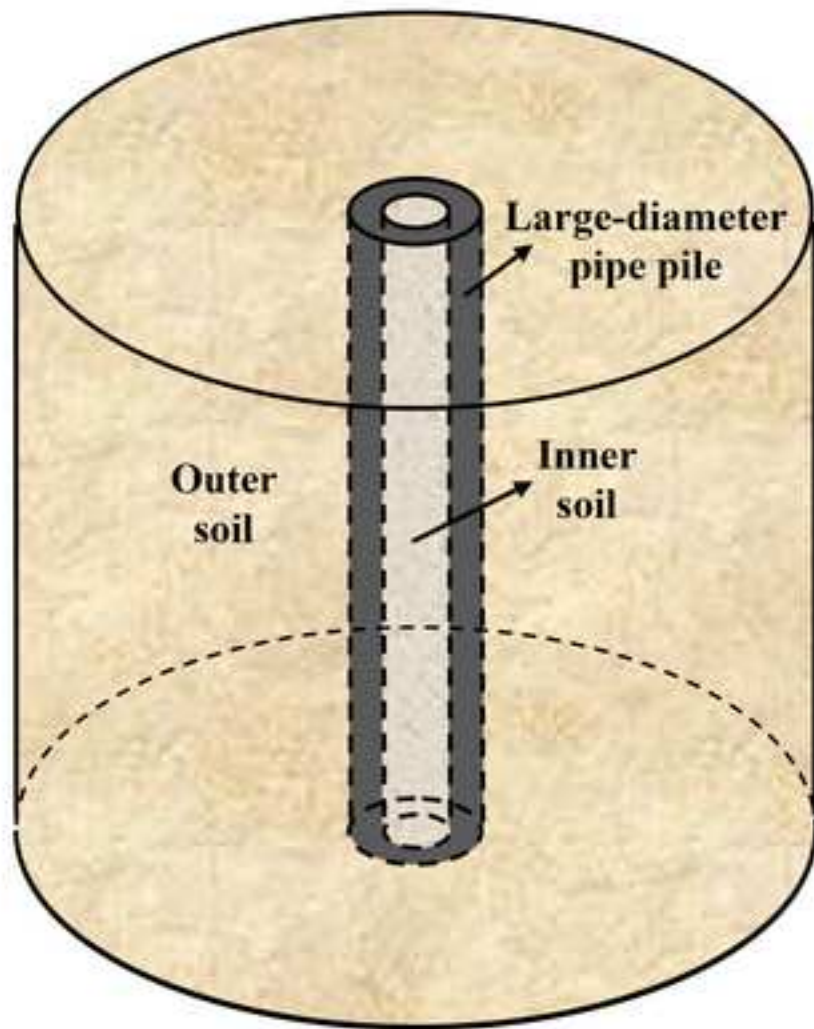


Fig.2(a)

[Click here to download high resolution image](#)

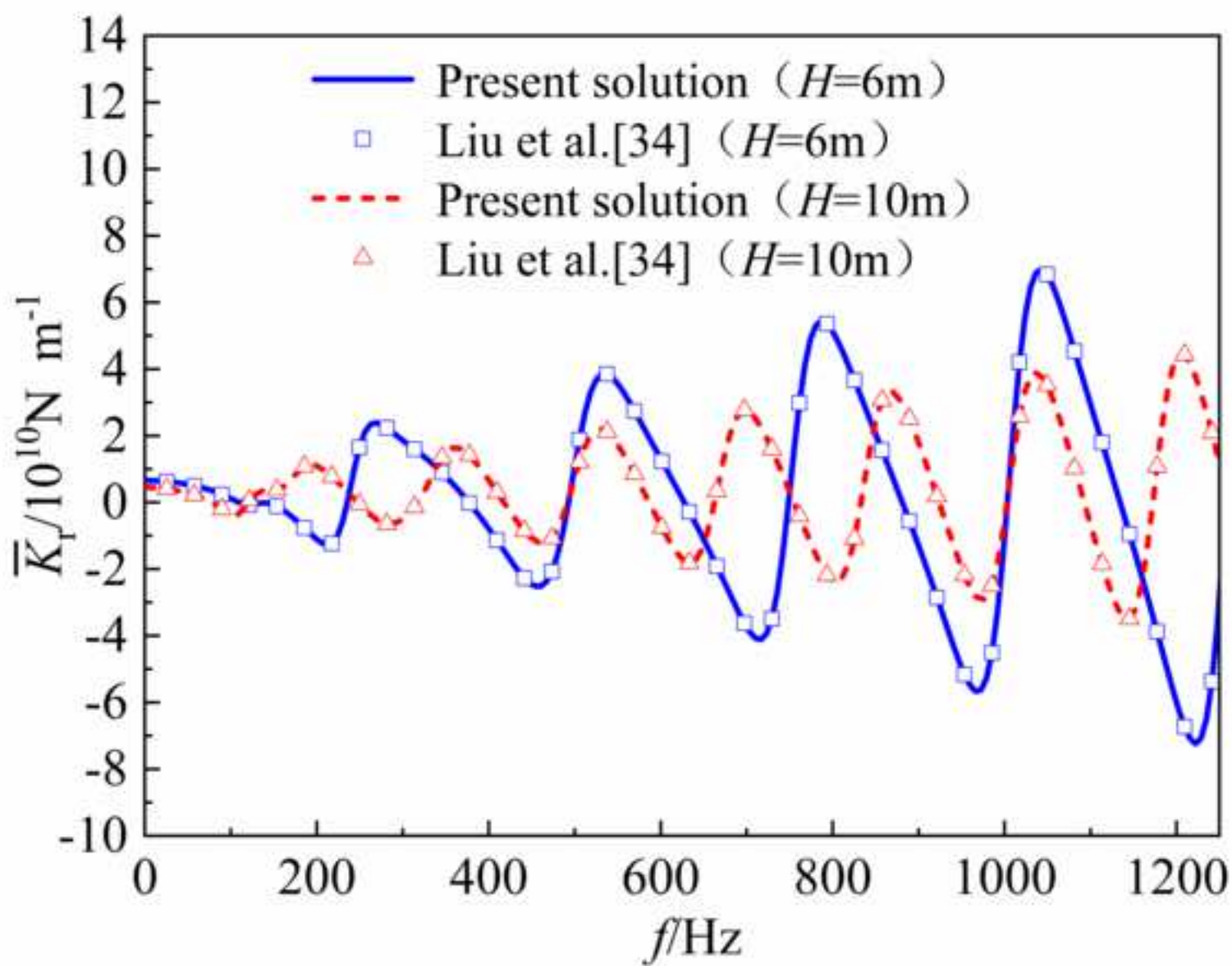


Fig.2(b)

[Click here to download high resolution image](#)

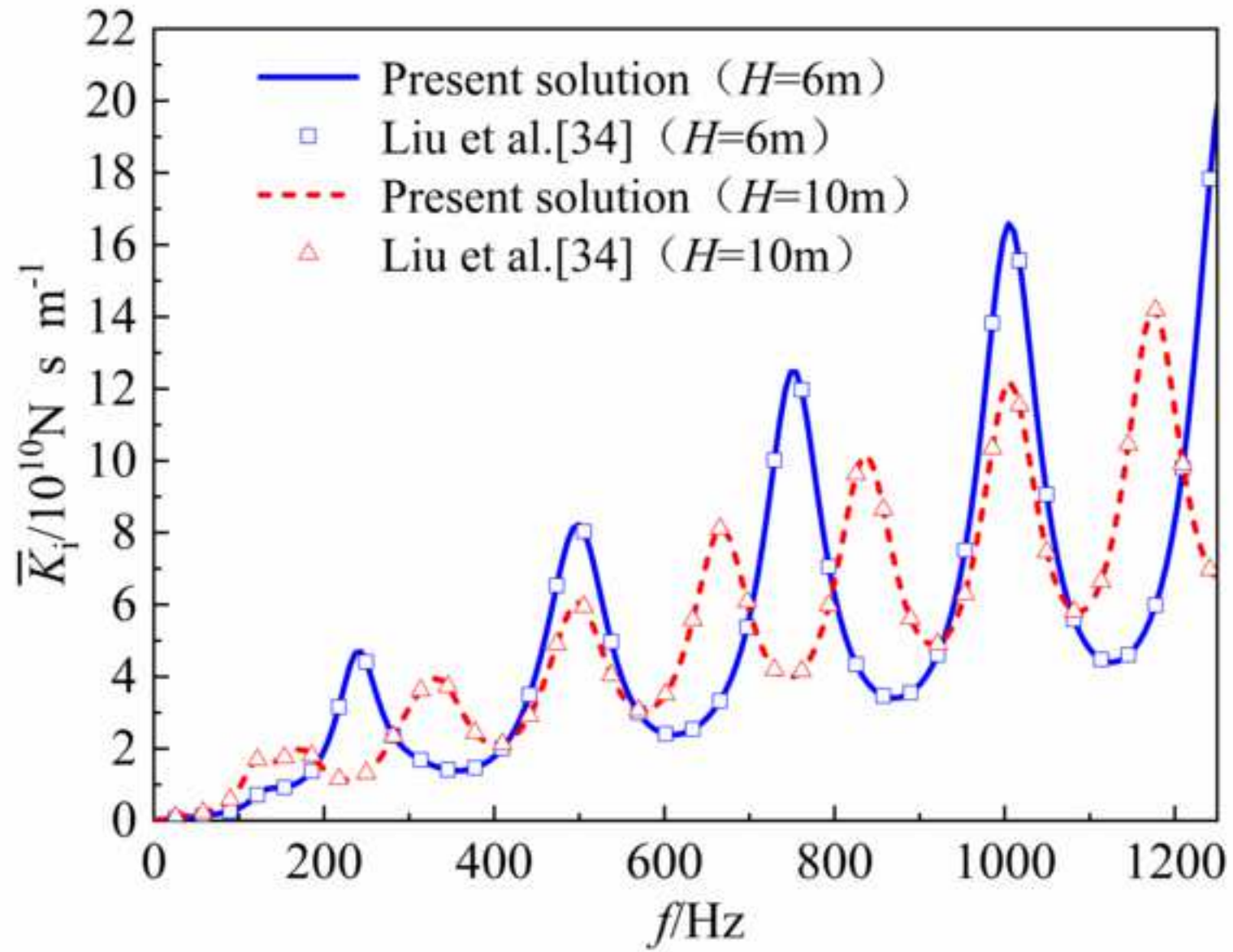


Fig.3(a)

[Click here to download high resolution image](#)

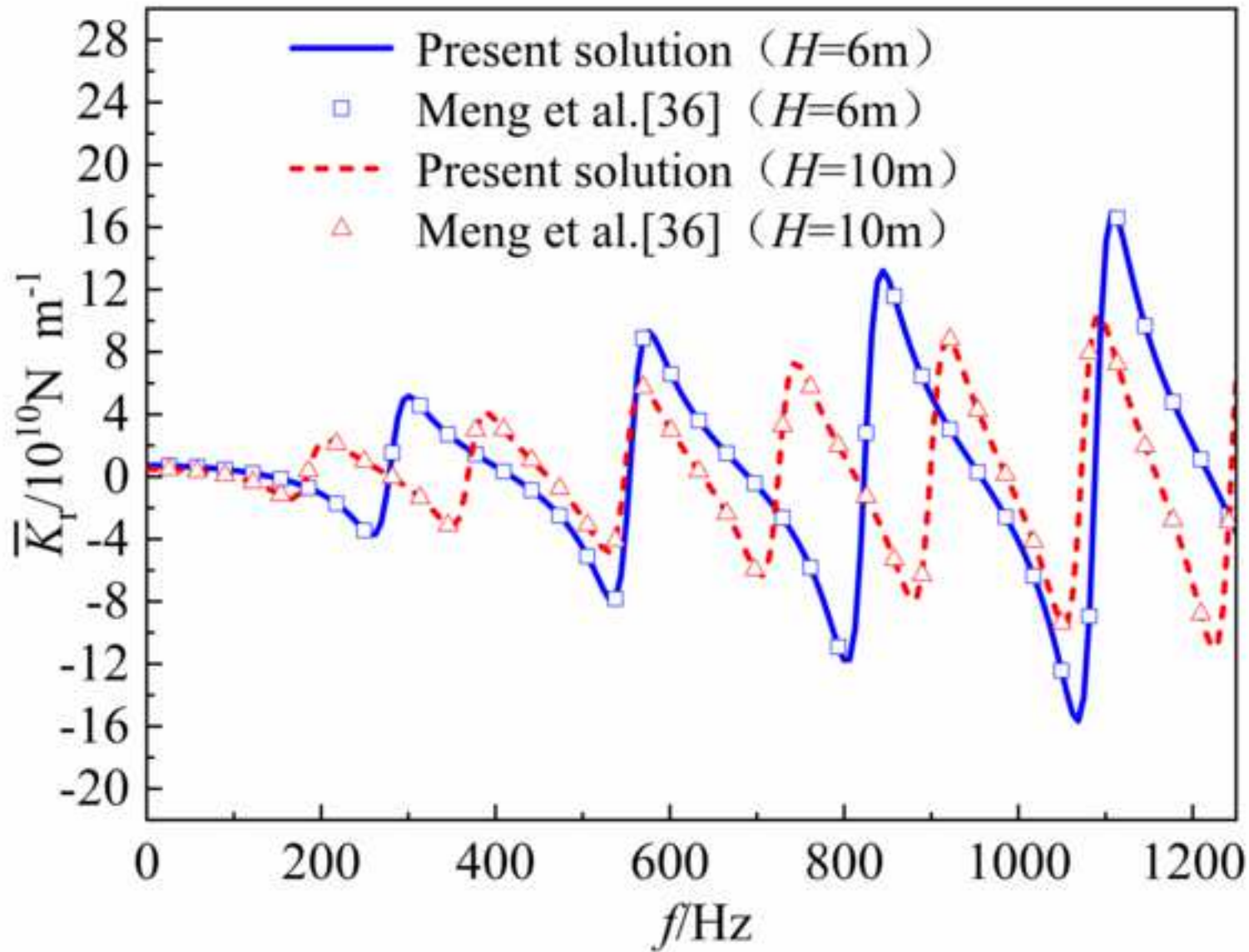


Fig.3(b)

[Click here to download high resolution image](#)

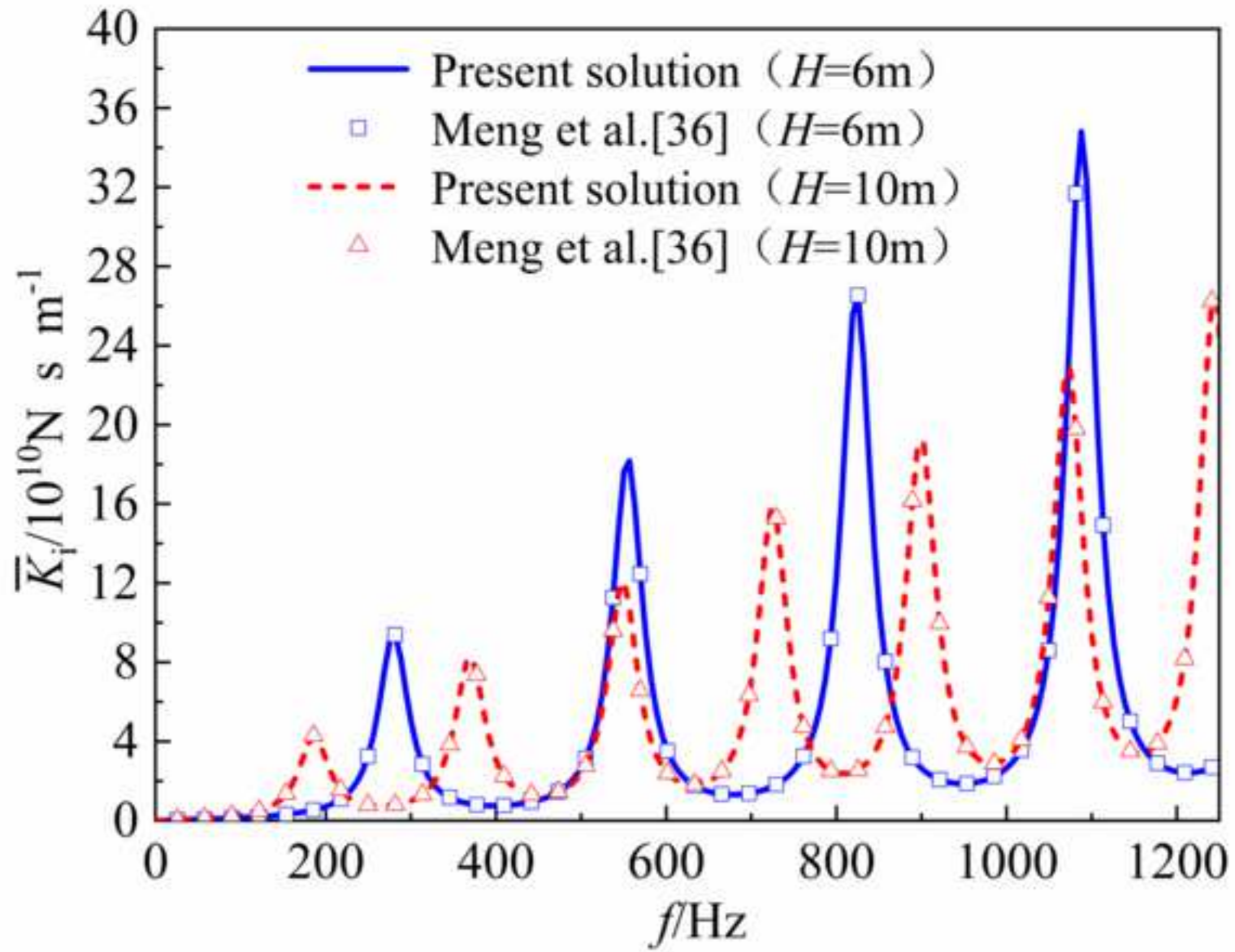


Fig.4(a)

[Click here to download high resolution image](#)

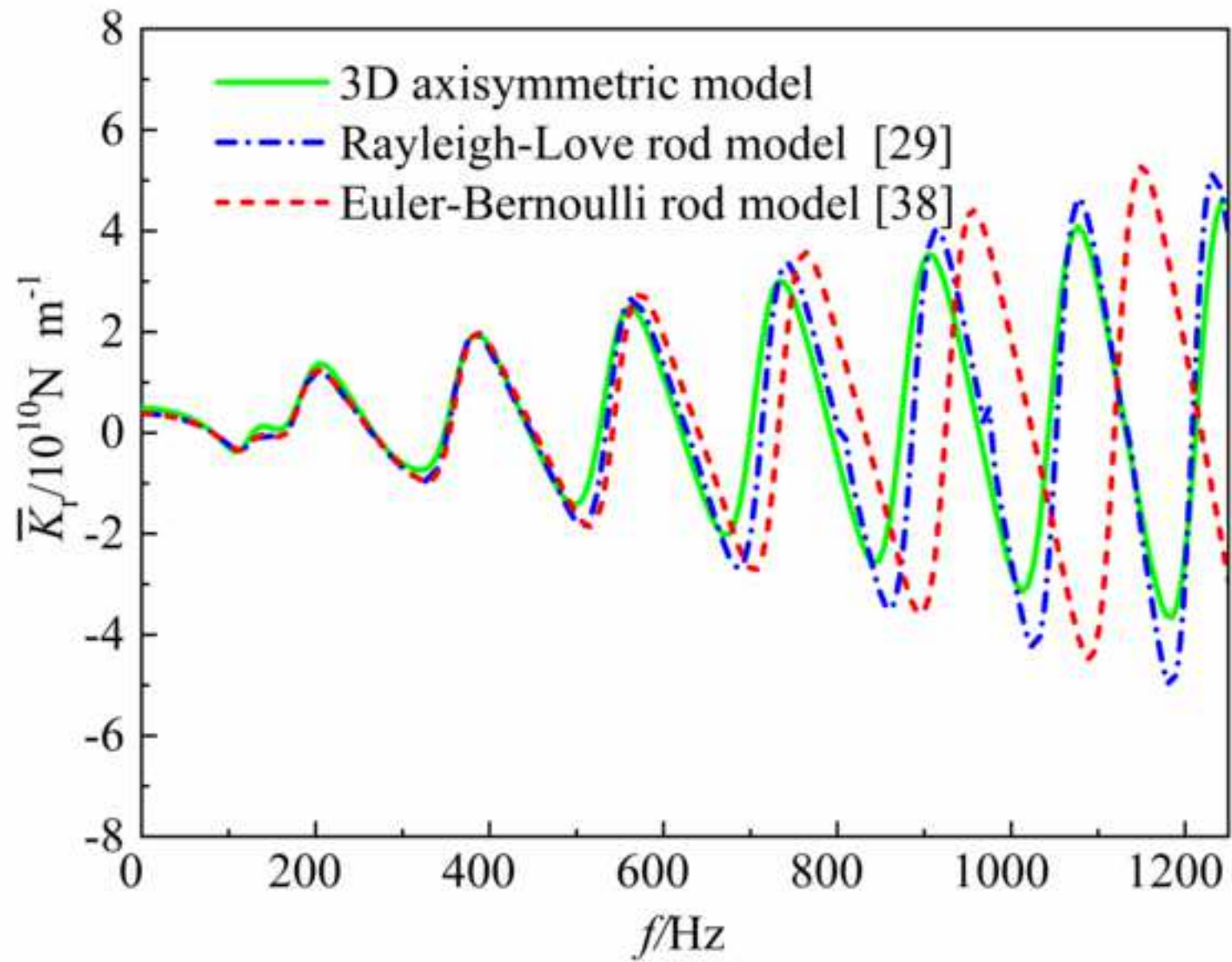


Fig.4(b)

[Click here to download high resolution image](#)

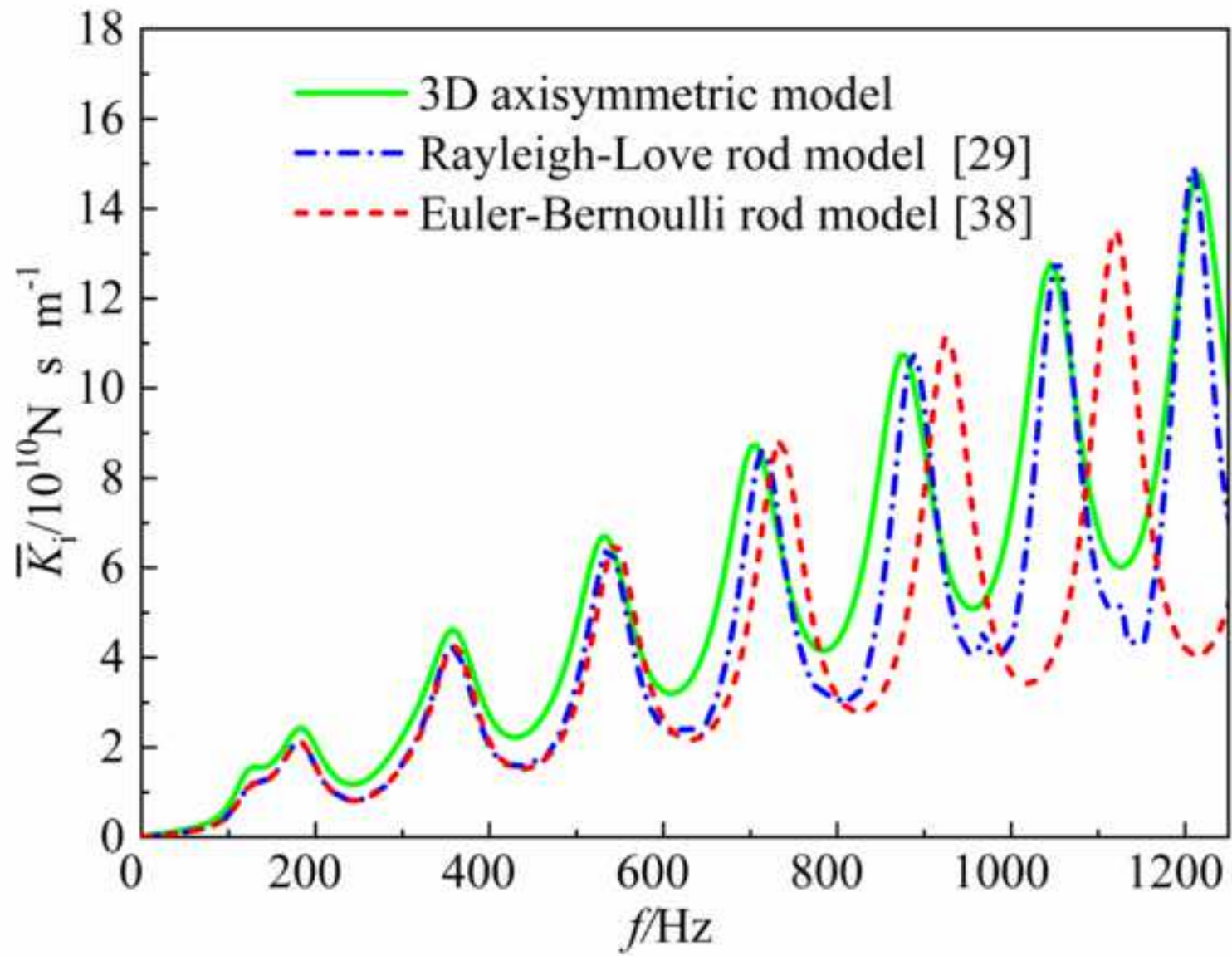


Fig.5(a)

[Click here to download high resolution image](#)

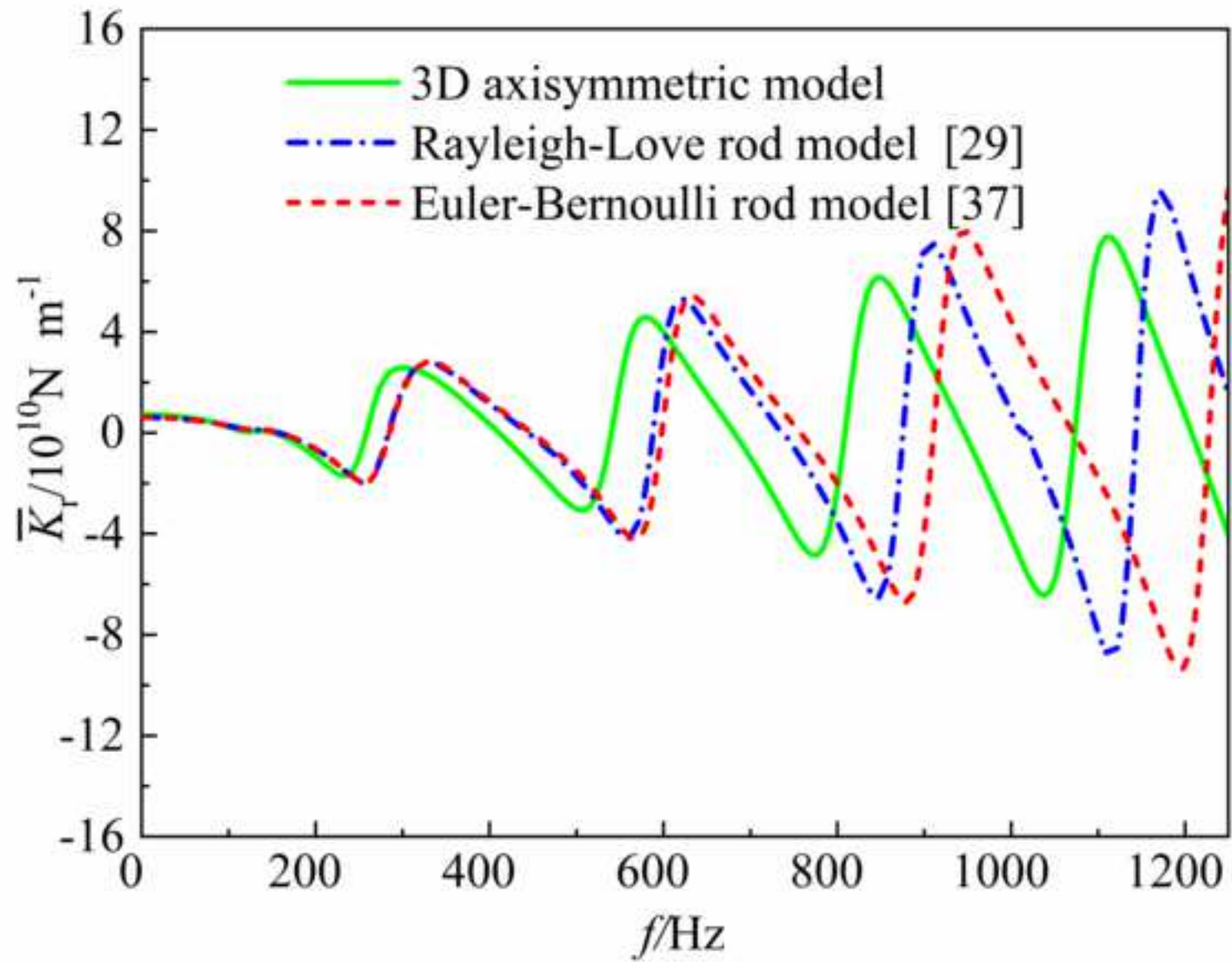


Fig.5(b)

[Click here to download high resolution image](#)

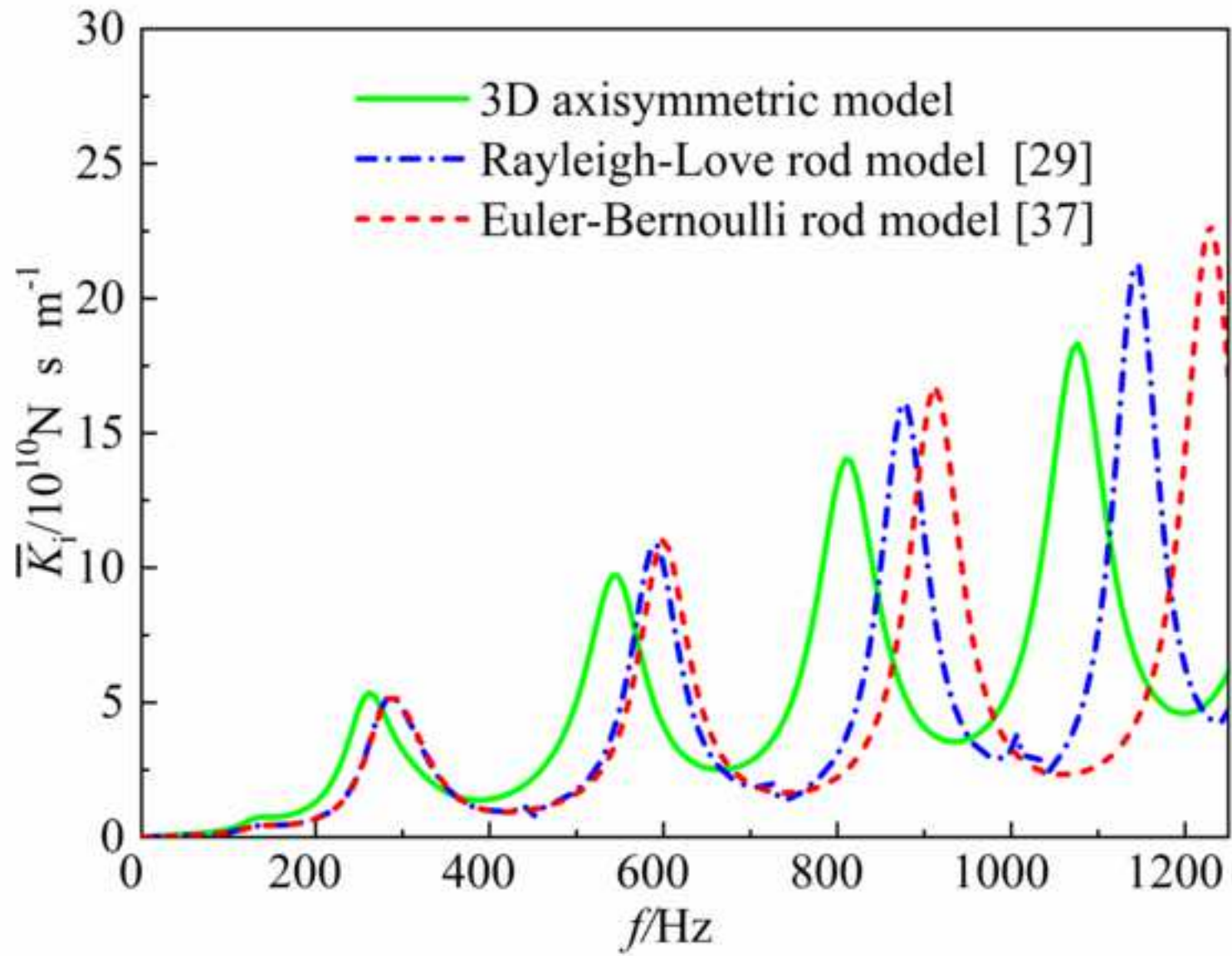


Fig.6
[Click here to download high resolution image](#)

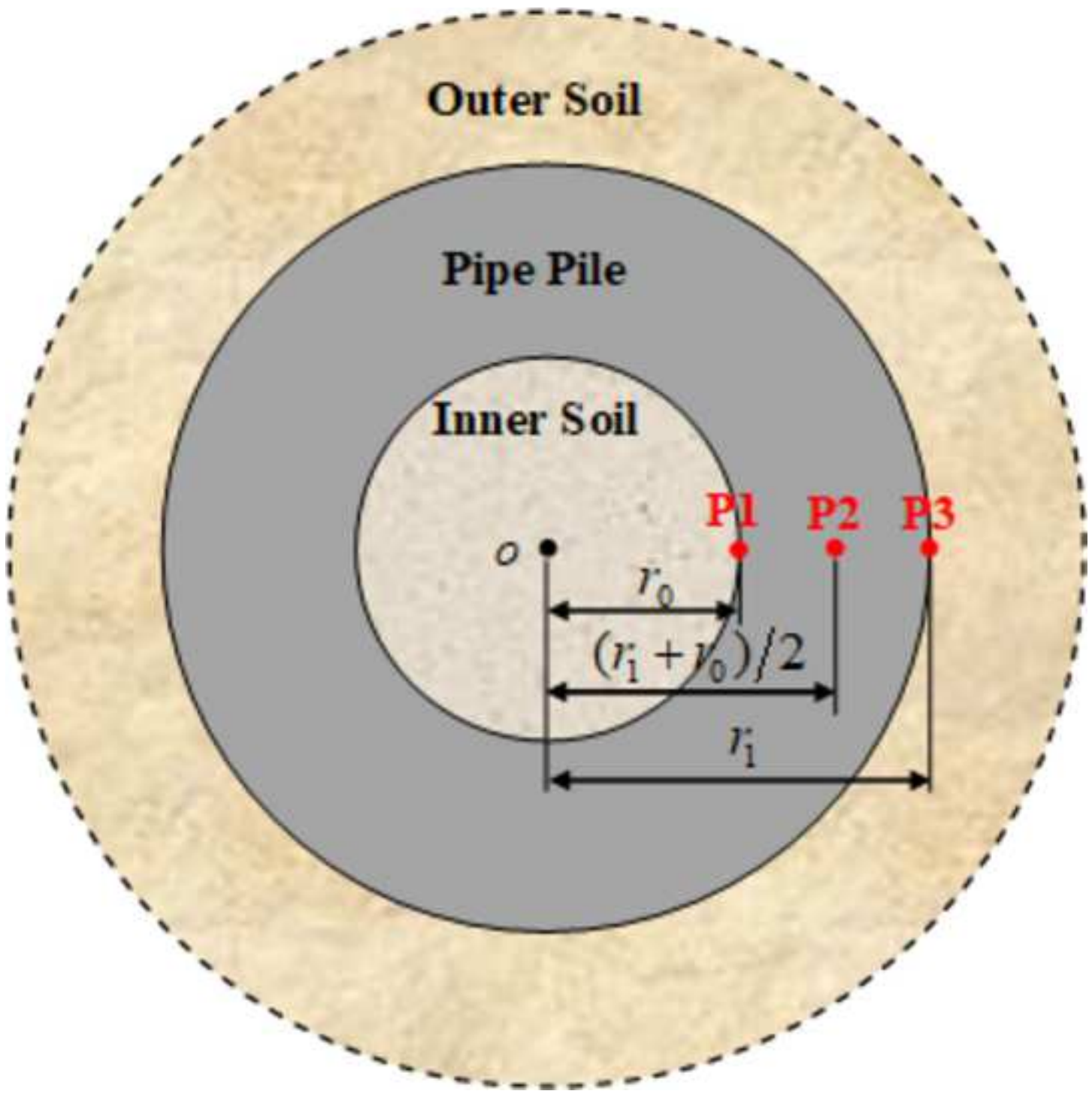


Fig.7(a)

[Click here to download high resolution image](#)

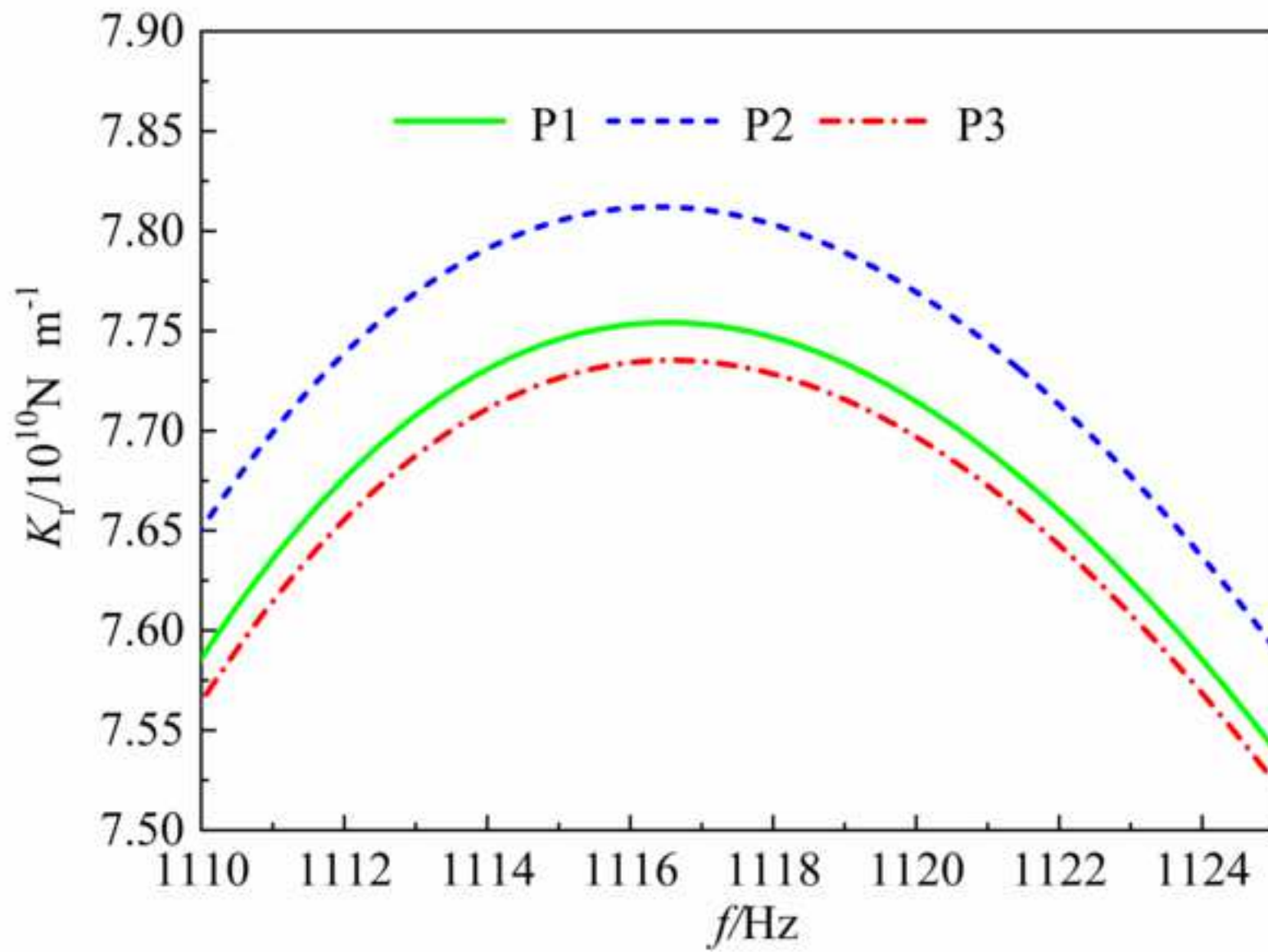


Fig.7(b)

[Click here to download high resolution image](#)

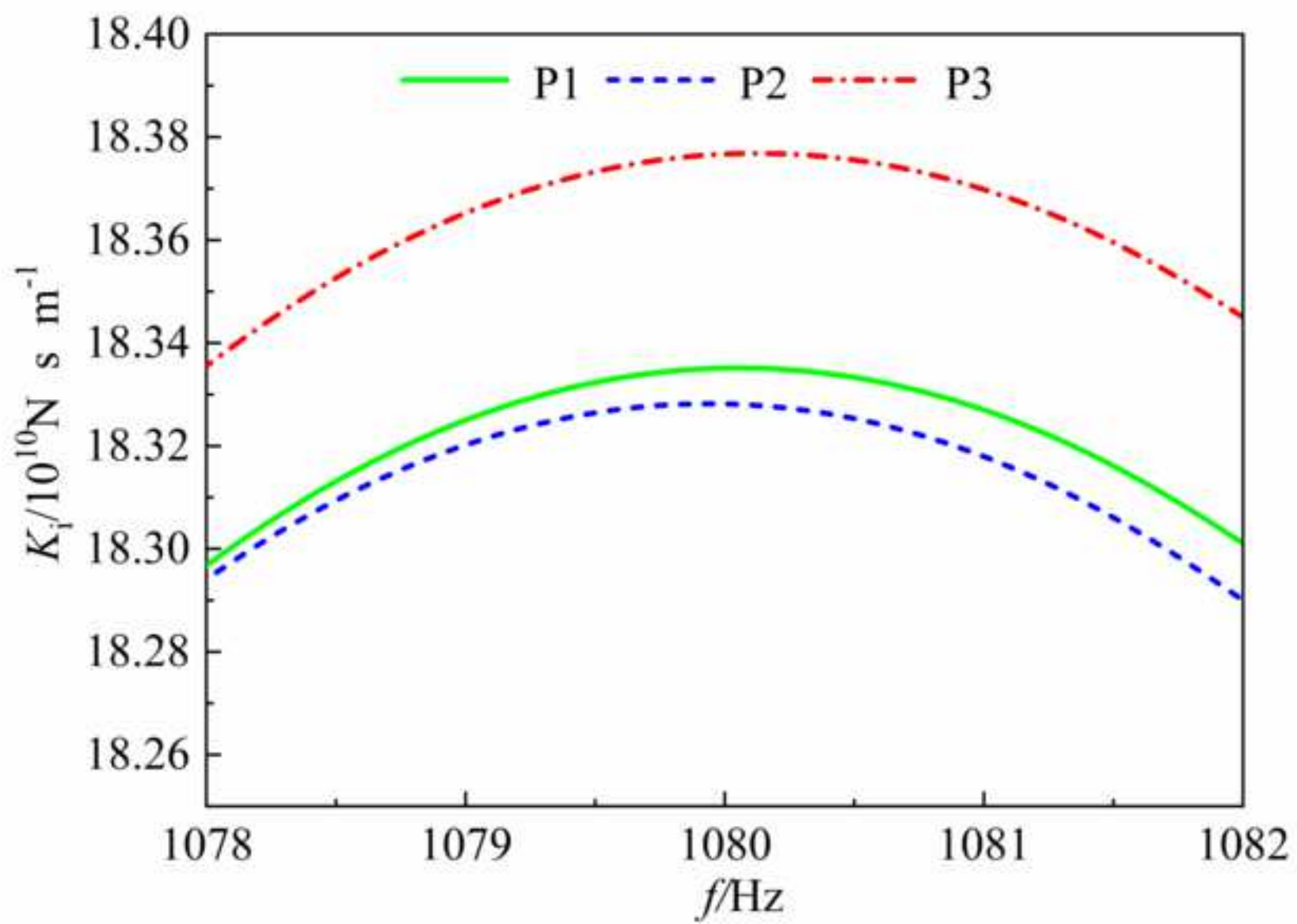


Fig.8(a)

[Click here to download high resolution image](#)

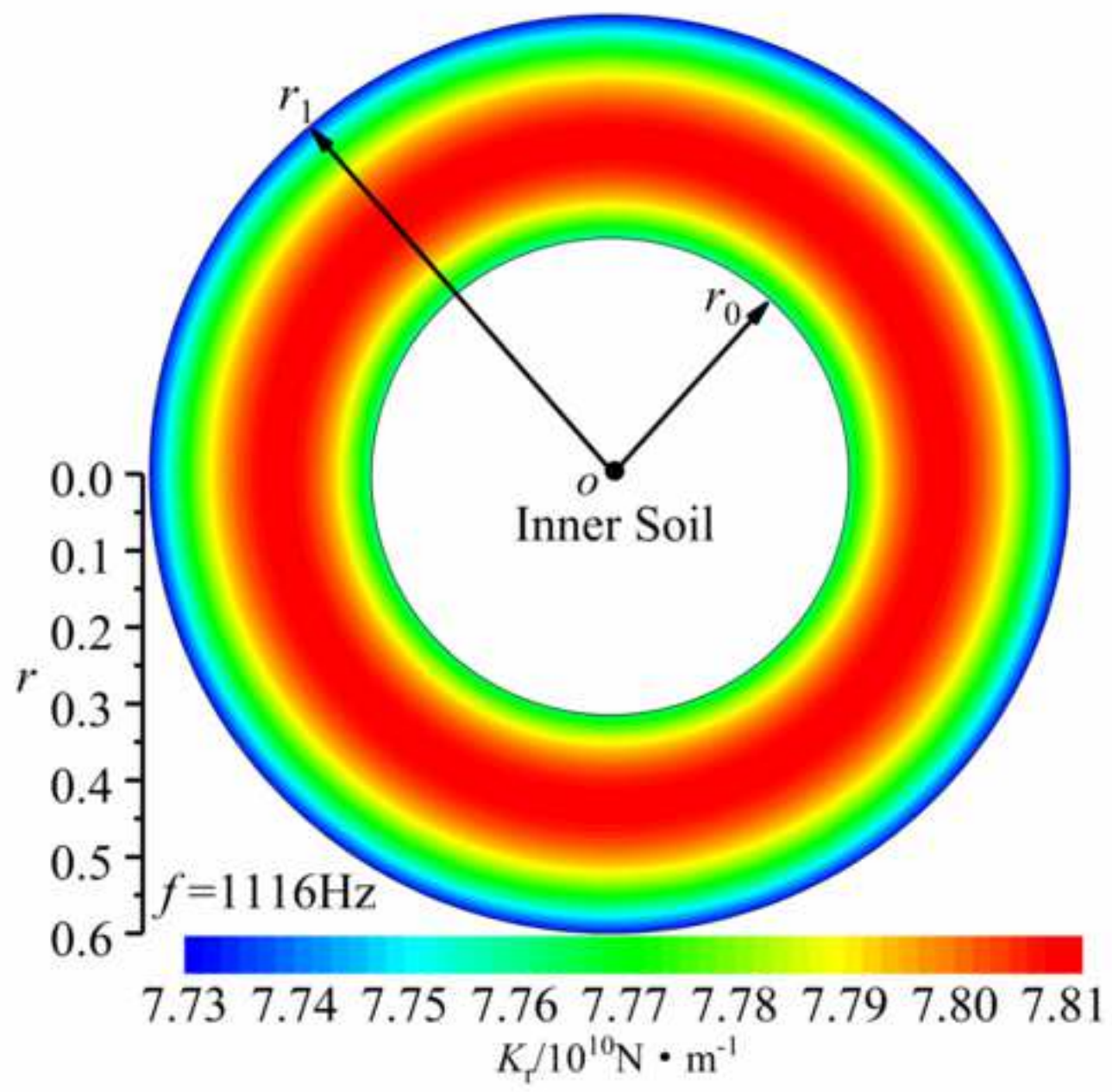


Fig.8(b)

[Click here to download high resolution image](#)

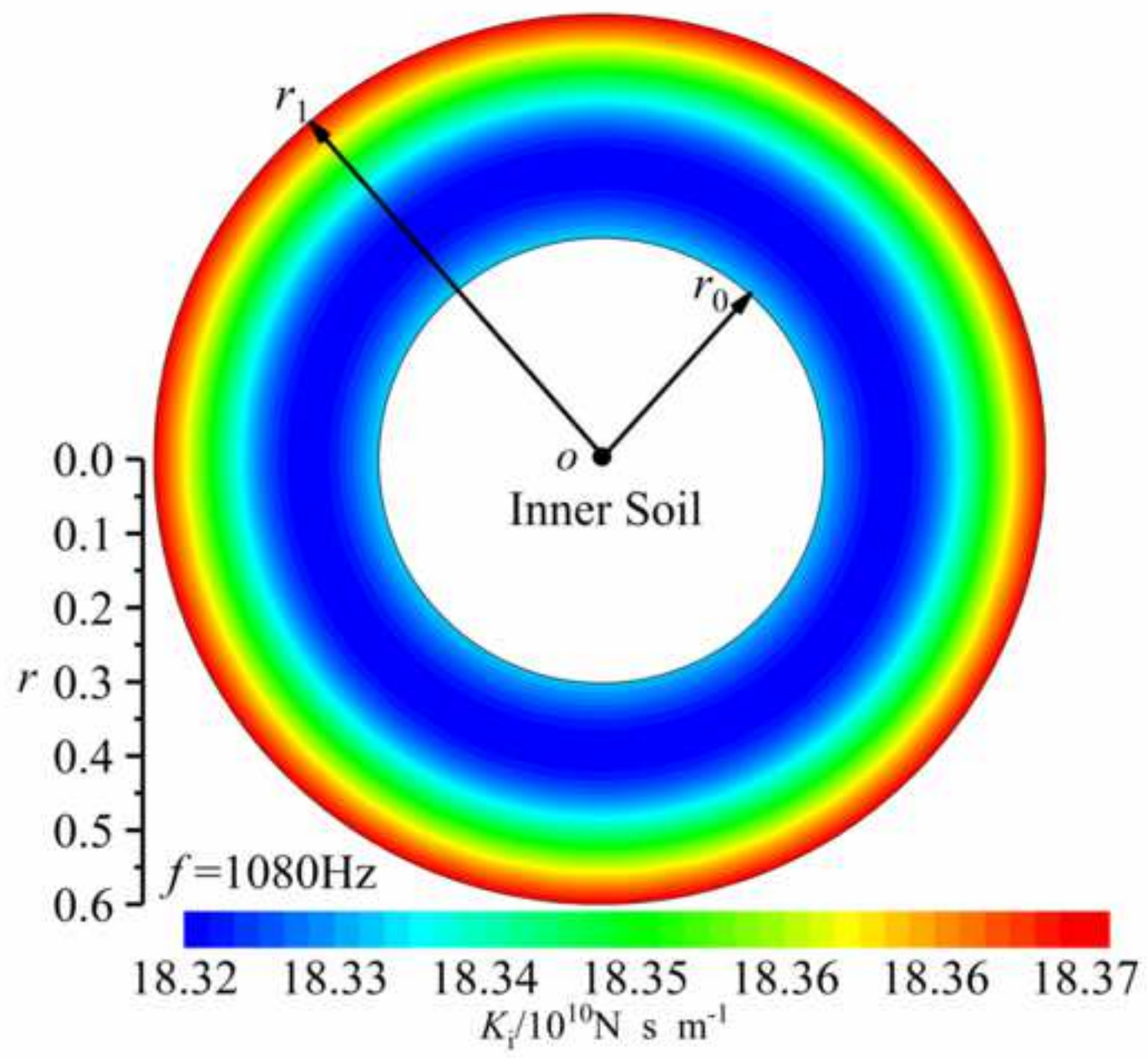


Fig.9(a)

[Click here to download high resolution image](#)

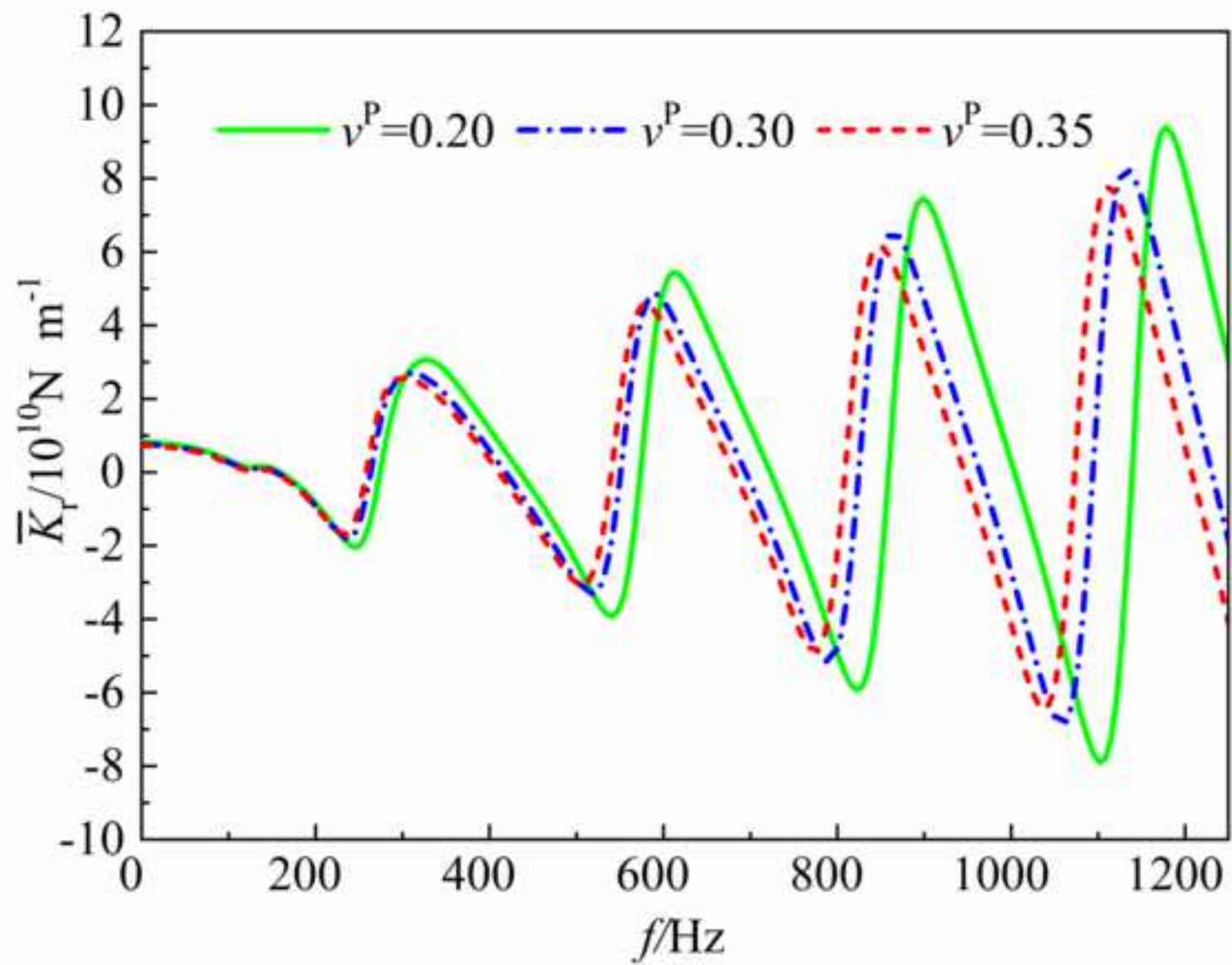


Fig.9(b)

[Click here to download high resolution image](#)

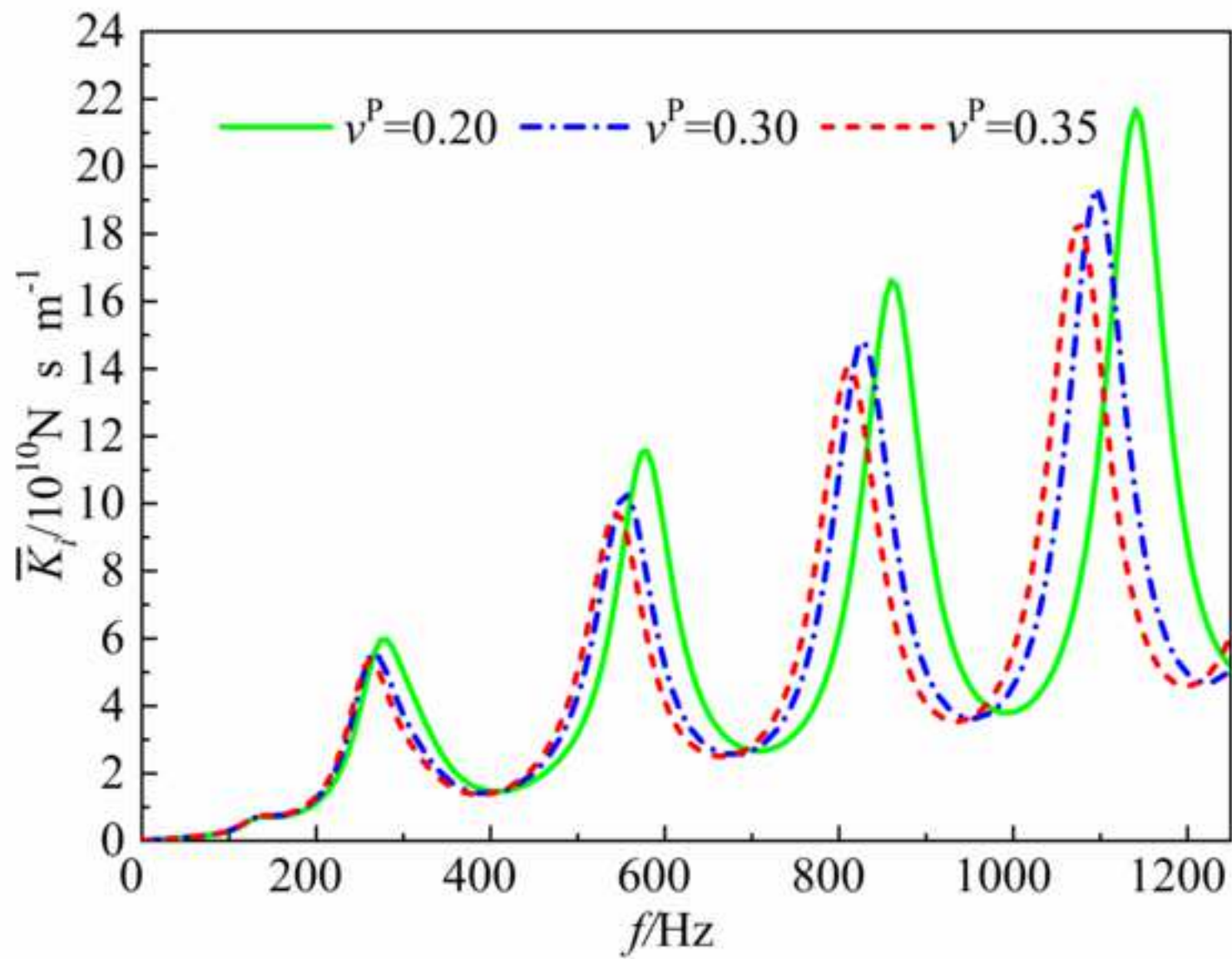


Fig.10(a)

[Click here to download high resolution image](#)

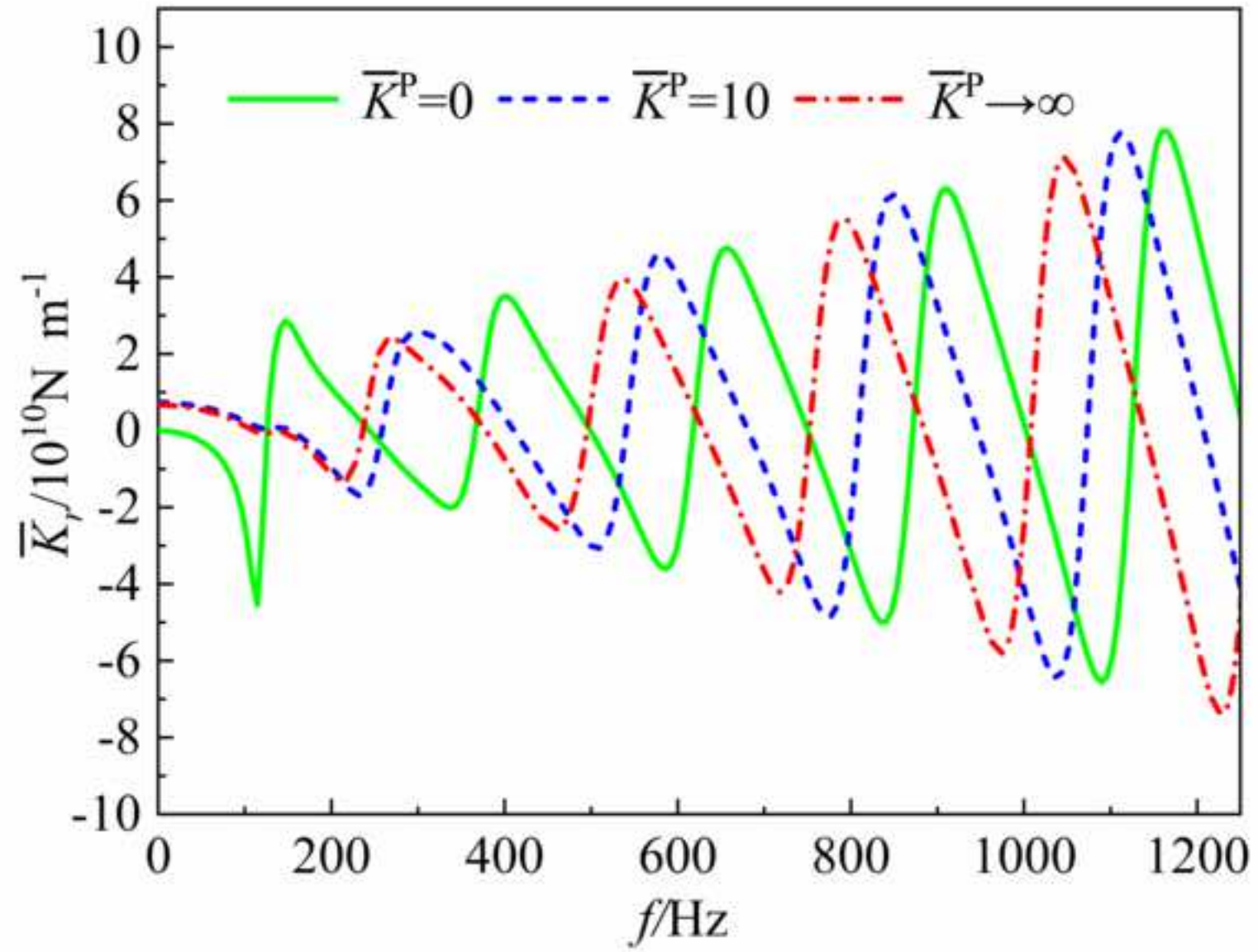
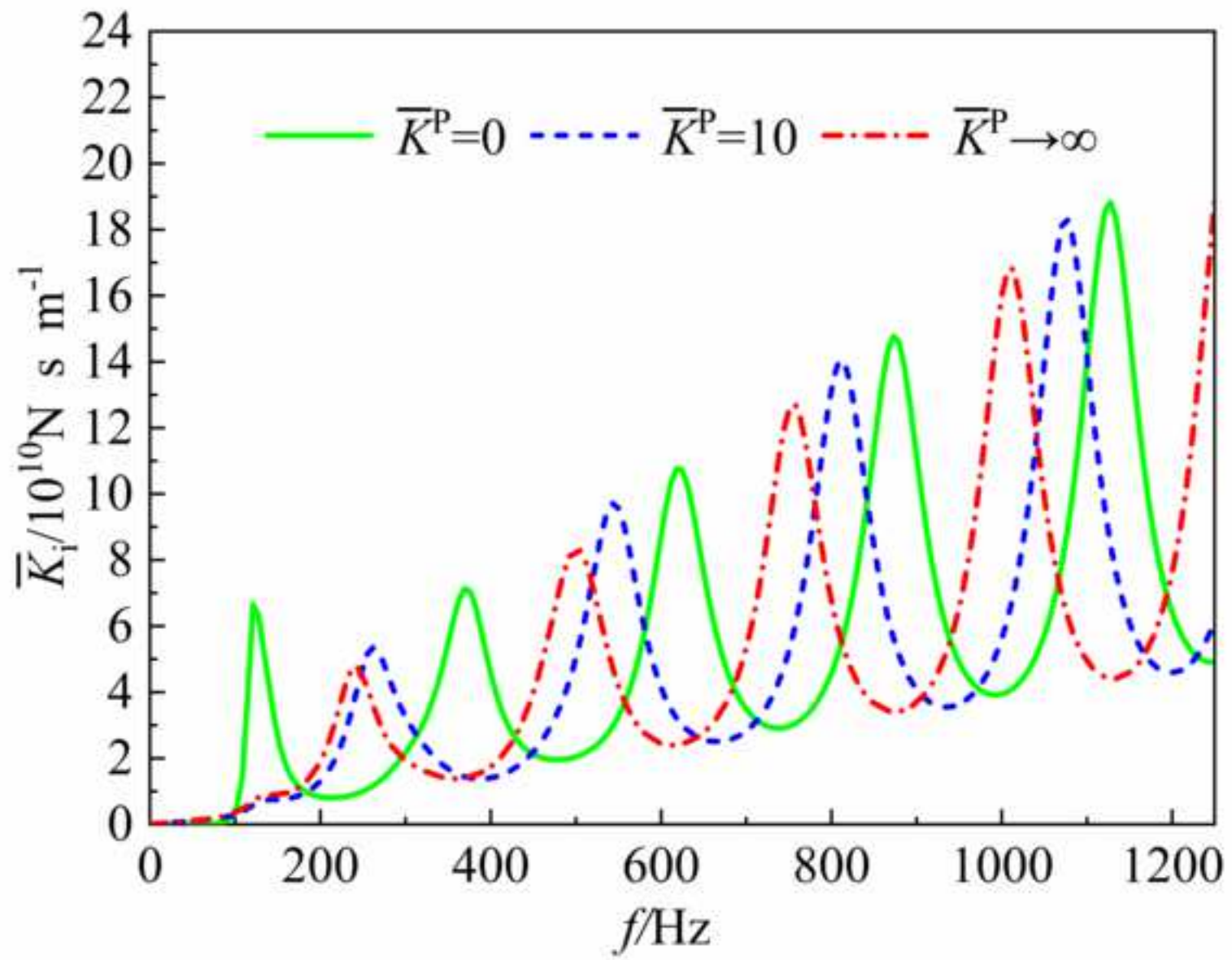


Fig.10(b)

[Click here to download high resolution image](#)



Highlights:

- (1) A novel approach is presented to describe the vertical vibration system of a large-diameter floating pipe pile and soils, considering the three-dimensional wave effects.
- (2) The proposed approach and corresponding solutions provide a more extensive scope of application and can be reduced for the vertical vibration problems of large-diameter floating solid pile and fixed-end pipe pile.
- (3) The limitations of previous solutions derived from rod-type models are demonstrated, which may lead to an overestimation of impedance, especially for piles with small slenderness ratio or high-frequency excitation.

Kun Meng: Conceptualization, Methodology, Software, Writing- Original draft preparation.

Chunyi Cui: Supervision, Writing-Reviewing and Editing, Resources, Formal analysis, Project administration, Funding acquisition.

Zhimeng Liang: Data curation, Investigation.

Haijiang Li: Supervision, Visualization.

Huafu Pei: Software, Validation.